AFRL-SR-AR-TR-02-

0 441

REPORT DOCUMENTATION PAGE

The public reporting burden for this collection of information is estimated to average 1 hour per response, including the tim gathering and maintaining the data needed, and completing and reviewing the collection of information. Send comments regar... of information, including suggestions for reducing the burden, to Department of Defense, Washington Headquarters Services, Directorate for Information Operations and Reports (0704-0188), 1215 Jefferson Davis Highway, Suite 1204, Arlington, VA 22202-4302. Respondents should be aware that notwithstanding any other provision of law, no person shall be subject to any penalty for failing to comply with a collection of information if it does not display a currently valid OMB control number.
PLEASE DO NOT RETURN YOUR FORM TO THE ABOVE ADDRESS.

1. REPORT DATE (DD-MM-YYYY)	2. REPORT TYPE	3. DATES COVERED (From - To)
10/12/2002	Final report	09/15/01-09/14/02

4. TITLE AND SUBTITLE	5a. CONTRACT NUMBER
"INVESTIGATION OF INTEGRATED COATING SYSTEM FOR CORROSION PROTECTION"	F49620-01-C-005?

5b. GRANT NUMBER

NA

5c. PROGRAM ELEMENT NUMBER

65502F NA

6. AUTHOR(S)	5d. PROJECT NUMBER
Parkhill, Robert M., Ph.D.	STTR NA
Kotov, Nicholas A., Ph.D.	5e. TASK NUMBER
Knobbe, Edward T. Ph.D.	TX NA

5f. WORK UNIT NUMBER

NA

7. PERFORMING ORGANIZATION NAME(S) AND ADDRESS(ES)	8. PERFORMING ORGANIZATION REPORT NUMBER
Sciperio, Inc. Oklahoma State University 5202 N Richmond Hill Rd Grants & Contracts Stillwater, Ok. 74075 402 Whitehurst Hall Stillwater, Ok.74078-1031	AF1-Final

9. SPONSORING/MONITORING AGENCY NAME(S) AND ADDRESS(ES)	10. SPONSOR/MONITOR'S ACRONYM(S)
AFOSR/NL Attn: Lt. Col. Paul Trulove 801 North Randolph Street, Room 732 Arlington, VA 22203-1977	NA
	11. SPONSOR/MONITOR'S REPORT NUMBER(S)
	NA

12. DISTRIBUTION/AVAILABILITY STATEMENT

Distribution Statement A: Approved for public release; distribution is unlimited.

20030115 104

13. SUPPLEMENTARY NOTES

NA

14. ABSTRACT

This report details the coasting systems developed under STTR contract for topic AF01-018. Coating systems comprising an inhibitor-doped layer-by-layer (LBL) assembly basecoat and a dense organically modified silicate (Ormosil) topcoat were investigated as corrosion-resistant coatings for 2024-T3 aluminum alloy. Neither the LBL nor the Ormosil materials were found to provide adequate corrosion protection for the underlying metal. A combination of the two coating methods was found to produce a synergistic enhancement in corrosion-resistance characteristics. Incorporation of an active corrosion inhibitor into the LBL coating was also found to improve corrosion-resistance properties. Zincate solutions were found to remove LBL/Ormosil coatings "on demand" from the aluminum-alloy substrate. All objectives set forth in the original Phase I project have been accomplished successfully, resulting in the development of an environmentally compliant protective coating that incorporates active corrosion inhibitors and that can be removed readily when needed.

15. SUBJECT TERMS

Corrosion Inhibitor; Release on Command; Barrier Coating; Sol-Gel; ORMOSIL; Nanocomposite; Layer-by Layer Assembly;

16. SECURITY CLASSIFICATION OF:			17. LIMITATION OF ABSTRACT	18. NUMBER OF PAGES	19a. NAME OF RESPONSIBLE PERSON
a. REPORT	b. ABSTRACT	c. THIS PAGE	SEE #12	41	Dr. Robert Parkhill
UNC	UNC	UNC			19b. TELEPHONE NUMBER (Include area code) 405/624-5751

Standard Form 298 (Rev. 8/98)
Prescribed by ANSI Std. Z39.18

INVESTIGATION OF INTEGRATED COATING SYSTEM FOR CORROSION PROTECTION

Principal Investigator: Dr. Robert L. Parkhill, Sciperio Inc.
Co-Principal Investigator: Dr. Nicholas A. Kotov, Oklahoma State University
Co-Principal Investigator: Dr. Edward T. Knobbe, Oklahoma State University and Sciperio Inc.
Report Prepared by Dr. Olga M. Kachurina, Sciperio Inc., and Dr. Tammy L. Metroke, Oklahoma State University

Abstract

Coating systems comprising an inhibitor-doped layer-by-layer (LBL) assembly basecoat and a dense organically modified silicate (Ormosil) topcoat were investigated as corrosion-resistant coatings for 2024-T3 aluminum alloy. As single-layer coatings, neither the LBL nor the Ormosil materials were found to provide adequate corrosion protection for the underlying metal. As determined using electrochemical techniques, a *combination* of the two coating methods was found to produce a synergistic enhancement in corrosion-resistance characteristics. Incorporation of an active corrosion inhibitor into the LBL coating was found to improve significantly its corrosion-resistance properties. The application of a dense Ormosil coating onto the inhibitor-exchanged LBL coating sealed the inhibitor ions into the LBL coating, thereby producing a reservoir of corrosion inhibitors in the direct vicinity of the metal substrate. The overlapping, anisotropic nature of clay platelets in the LBL coating slowed the migration of corrosion initiators that may have breached the integrity of the Ormosil layer, while enabling the lateral diffusion of the inhibitor to the defect site. Two methods were investigated by which to remove the LBL/Ormosil coating systems from the aluminum-alloy substrate. Zincate solutions were found to remove effectively and rapidly LBL/Ormosil coating systems from the metal

substrate, leaving a thin zincate product layer. Dilute oxalate solutions were found to remove LBL assemblies and to provide corrosion protection for the underlying metal.

Publications Stemming from this Research Effort

1. "Ecologically Benign Corrosion Protection with Nanostructured Thin Films," Olga Kachurina, Tammy L. Metroke, John W. Ostrander, Nicholas A. Kotov, and Edward T. Knobbe, to be submitted to *Chemistry of Materials*.

2. "Investigation of Integrated Coating System for Corrosion Protection," R. L. Parkhill, O. Kachurina, T. L. Metroke, J. Ostrander, and N. Kotov. Presented at the Triservice Conference, January 2002.

3. "Corrosion Protection of Aluminum Sheets by Composite Layer-by-Layer Assembly," J. Ostrander, O. Kachurina, T. L. Metroke, E. T. Knobbe, and N. A. Kotov. Presented as a poster at the 223rd National Meeting of the American Chemical Society, Orlando, Florida, 2002.

Table of Abbreviations and Symbols

A	Area, Electrode Surface (cm^2)		NMR	Nuclear Magnetic Resonance
AA	Aluminum Alloy		Ormosil	Organically Modified Silicate
ACI	Active Corrosion Inhibitor		PAA	Poly(acrylic acid)
c	Concentration (vol %)		PDDA	Poly(diallyldimethyldiammonium chloride)
C_c	Capacitance, Coating (F/cm^2)		PDS	Potentiodynamic Scan
C_{dl}	Capacitance, Double-Layer (F/cm^2)		PE	Polyelectrolyte
CP	Cross-Polarized, -Polarization (NMR)		R_{corr}	Resistance, Corrosion ($\Omega \cdot cm^2$)
d	Thickness, Coating (cm)		R_{po}	Resistance, Pore ($\Omega \cdot cm^2$)
E_{corr}	Potential, Corrosion (V)		R_{pol}	Resistance, Polarization ($\Omega \cdot cm^2$)
E_{oc}	Potential, Open Circuit (V)		R_{tot}	Resistance, Total ($\Omega \cdot cm^2$)
E_{pit}	Potential, Pitting (V)		R_u	Resistance, Solution ($\Omega \cdot cm^2$)
EIS	Electrochemical Impedance Spectroscopy		SEM	Scanning Electron Micrograph
f	Frequency (Hz)		t_{cr}	Time, Coating Removal (s)
J_a	Current Density, Anodic (A/cm^2)		t_i	Time, Immersion (s)
J_{corr}	Current Density, Corrosion (A/cm^2)		T_r	Temperature, Room or Ambient (°C)
LBL	Layer-by-Layer		TEOS	Tetraethoxysilane or Tetraethyl Orthosilicate
M	Molar (mol/L)		VTMOS	Vinyltrimethoxysilane
MAS	Magic-Angle Spinning (NMR)		Z	Impedance ($\Omega \cdot cm^2$)
MEMO	3-(Trimethoxysilyl)propylmethacrylate		ε_0	Dielectric Constant, Absolute (F/m)
MW	Molecular Weight (Da)		ε_r	Dielectric Constant, Relative (−)
n	Number (−)		φ	Angle, Phase (deg)

I.   LBL/Ormosil Coating Systems

A.   Introduction

The U.S. Air Force is presently facing a critical need to develop environmentally compliant surface treatments designed to mitigate corrosion of aircraft aluminum alloys (AA's). Currently available surface pretreatments for AA's have been determined to comprise human and environmental health hazards (*e.g.*, hexavalent-chromium-based conversion coatings) and/or to exhibit limited effectiveness as corrosion inhibitors.   The goal of the proposed project is to prepare and evaluate advanced hybrid coatings that:

- Are environmentally compliant;

- Serve as an effective barrier layer that is readily incorporated into a multilayer paint system;

- Contain a reservoir of nanoengineered structures targeted to provide electrochemically active corrosion inhibitors "on demand" in the case of a barrier-layer breach; and

- Release (*i.e.*, separate from the substrate) "on command."

In recent years, a wide variety of novel coating processes have been developed as potential replacements for hexavalent-chromium-based conversion coatings as described in various reviews [1–3]. These processes have relied on inorganic molecules that react with the oxidized aluminum surface to form mixed oxides, metal ions that are able to oxidize the metal surface during service life, organic polymers with a high complexing capacity for aluminum surfaces, and inorganic-film-forming oxides [4]. Recent developments have included rare-earth-based conversion coatings [5], Co-rich oxide layers [6], Mn-based conversion coatings [7], Mo-based conversion coatings [8], Zr-based conversion coatings [9], silane-based surface treatments [10–11], and Cr^{3+}-based conversion coatings [12].

Coatings derived from organically modified silicate (Ormosil) materials [13] have found use in a diverse range of high-performance applications, including enhancement of mechanical,

thermal, optical, corrosion-resistance, and electrical properties of the underlying materials [14]. Organically modified silicate (Ormosil) coatings have been found to provide good corrosion resistance for metal substrates based on their ability to form dense barriers to the penetration of corrosion initiators [11, 15]. Review articles by Guglielmi [16], Knobbe *et al.* [17], and Twite and Bierwagen [3] indicate that sol–gel-derived coatings are of interest for improving corrosion resistance of various metallic substrates.

In general, the corrosion-resistance behaviors of sol–gel-derived coatings are based on the ability of the coatings to provide excellent barriers to the penetration of corrosion initiators. In order to enhance the coating corrosion-resistance characteristics, it is necessary to introduce an *active corrosion inhibitor* (ACI) into the coating system to provide a secondary mechanism of corrosion protection in addition to the protective-barrier properties of the Ormosil. However, the high density of the Ormosil coating, which provides its good barrier properties, may inhibit the migration of ACI's through the coating, thereby limiting their effectiveness. Therefore, it is desirable to introduce a reservoir of ACI's into the system—preferably in the immediate vicinity of the metal surface—which are immobilized on a suitable substrate layer in the absence of reactions leading to general or localized corrosion.

Layer-by-layer (LBL) film assembly has been used to prepare coatings derived from a variety of oppositely charged polyelectrolytes (PE's) [18] with other species such as proteins [19], conducting polymers [20], zirconium phosphate [21], dyes [22], metal nanoparticles [23], semiconductor quantum dots [24], aluminosilicates [25], and graphite oxide [26] onto various substrate materials. LBL assembly involves the adsorption of polycations and polyanions from solutions of charged species onto an oppositely charged substrate. Subsequent repetitive application, rinsing, and drying of the growing film onto alternatively charged PE's allows the

buildup of a LBL-assembled multilayer coating system. The LBL assembly process is governed by adsorption and desorption equilibria of species with appropriate hydrophobicities, charges, and charge densities.

Previous work has shown that the introduction of various clays into LBL assemblies provide coatings with useful properties. For example, Kleinfeld and Ferguson prepared LBL assemblies of poly(diallyldimethyldiammonium chloride) (PDDA) and exfoliated sheets of synthetic hectorite, a mica-type layered silicate on Si wafers [27]. Kotov *et al.* investigated the morphology and gas permeation of montmorillonite–PE self-assembled multilayer systems on poly(ethyleneterephthalate) as highly selective ultrathin membranes [28]. At this time, the corrosion-resistance characteristics of LBL-derived coatings have not been fully investigated. However, advantages of LBL coatings for corrosion resistance include the simplicity of the deposition procedure, control of the average thickness of the PE layers, the ability to produce dense layers, and the ability to exchange corrosion-inhibiting ions.

In this study, the preparation and corrosion-resistance characteristics of multilayer LBL/Ormosil coatings on 2024-T3 aluminum alloy were investigated. Experimental results indicate that the investigated LBL/Ormosil system had the potential to enhance significantly the corrosion-resistance characteristics of the underlying metal substrate. In this study, a multilayer system was prepared in which an absorbent, ion-exchangeable LBL-assembled underlayer is exchanged with an ACI. The ACI-doped layer is then sealed with a protective Ormosil coating. This coating system provides two mechanisms of corrosion protection. First, the dense Ormosil layer provides primary barrier protection. In the event that the integrity of the Ormosil layer is breached, the ion-exchanged LBL coating provides a reservoir of ACI's. At the onset of corrosion, the ACI molecules may migrate through the underlayer to the corrosion site, thereby

providing active corrosion protection in a dense coating system. Importantly, nanocomposite LBL coatings also provide a barrier function to the perpendicular movement of ACI's; however, they provide for the lateral diffusion responsible for rapid delivery of ACI's to defect sites.

B. Experimental

1. Materials

Tetraethoxysilane or tetraethyl orthosilicate (TEOS), 3-(trimethoxysilyl)propyl-methacrylate (MEMO), and vinyltrimethoxysilane (VTMOS) were purchased from Aldrich or Gelest and were used as received. Swy-2 sodium montmorillonite (University of Missouri–Columbia, Source Clay Minerals Repository) was used as received without further purification. Poly(acrylic acid) (PAA), molecular weight (MW) ≈ 450 kDa, and poly(diallyldimethyldiammonium chloride) (PDDA), MW ≈ 400–500 kDa, were purchased from Aldrich and used as received.

2. Aluminum Surface Preparation

Substrate materials were 2024-T3 aluminum alloys (AA's). Test pieces were first wiped with hexanes and subsequently with methanol to reduce the concentration of residue from the manufacturing process, as well as any debris. Samples were placed in covered glass containers containing acetone and ultrasonicated (Fisher Scientific FS20) for approximately 45 minutes, then removed from the solution and allowed to dry at ambient conditions.

3. Preparation of Coating Solutions

A "clay solution" was prepared by dispersing approximately 1.5 g of clay in about 200 mL of deionized water followed by ultrasonication for 45 min. The solution was added to 800 mL of deionized water and shaken vigorously to promote dissolution of the clay material. The "PDDA coating solution" was a 1% aqueous solution of PDDA. The "PAA coating solution" was a 1% aqueous solution of PAA.

4.   Layer-by-Layer Assembly Preparation

In order to prepare LBL assemblies, the AA substrates were sequentially immersed in a PDDA solution for 5 min. to allow for good adsorption of the PE. The samples were removed from the PDDA solution and briefly rinsed with clean water from a plastic squeeze bottle to remove excess PE from the surface and edges. Subsequently, the samples were then transferred to another beaker containing clean water where they were rinsed for an additional 5 min. The samples were then transferred to a beaker containing a PAA solution, where the PE was allowed to adsorb for 5 min. The rinsing process was repeated, and the samples were immersed one more time for 5 min. in PDDA and then rinsed again. The wet samples were immersed in the clay suspension for 5 min.

This process was repeated for up to $n = 20$ layers, with visually apparent buildup of PE and clay after only $n = 4$ layers. The production of coatings composed of $n \geq 7$ layers may not be accomplished in one single experiment. Between layers, after the clay step and rinse, as required, the samples were dried with compressed air to remove as much water as possible and placed on end in a clean, dry, closed container. The experiment was then resumed in the following session. This interruption was not found to affect the sample quality.

5.   Sol–Gel Coating Preparation

Ormosils were prepared by mixing 5.6 mL of TEOS, 7.6 mL of VTMOS, 2.0 mL of MEMO, and 9.8 mL of 0.05-molar (M) HNO_3. The reaction mixtures were stirred for one hour prior to film deposition. The resultant Ormosil solutions were deposited onto cleaned or LBL-coated AA's by a spray-coating technique using an airbrush setup. The coatings were allowed to dry at ambient conditions for at least 24 hours prior to their characterization.

6.   Corrosion Inhibitors

In order to prepare inhibitor-doped layers, LBL-coated test coupons were immersed in 0.25-M $K_2Cr_2O_7$ for 30 min. at room or ambient temperature (T_r) or into a conversion-coating solution developed by Schriever [29] in order to introduce Cr^{6+} or Co^{3+} inhibitor ions, respectively. The Schriever conversion-coating solution was prepared by mixing 55 g/L of NH_4NO_3, 26 g/L of $Co(NO_3)_2 \cdot 6H_2O$, and 26.4 g/L of $HCOOH$ in 750 mL of H_2O. The pH of this solution was adjusted to 7.0–7.1 with concentrated NH_4OH. Subsequently, 3.5 mL/L H_2O_2 (30 wt. %) and distilled H_2O were added to increase the volume to 1 L. The stock solution was heated to 140 °F (60 °C) for 30–90 min. The final pH was adjusted to 6.8–7.0 using concentrated NH_4OH. Prior to use, the stock solution was allowed to cool to T_r. After immersion in the inhibitor solutions, the test coupons were rinsed with deionized water.

7.   Potentiodynamic Scan and Electrochemical Impedance Spectroscopy

Potentiodynamic scan (PDS) and electrochemical impedance spectroscopy (EIS) were used to evaluate the protective properties of investigated coatings. Detailed descriptions of these electrochemical methods can be found elsewhere [30]. Each coating system was evaluated in triplicate. Electrochemical measurements were performed using a Gamry PC3/300 potentiostat with Gamry Corrosion Measurement System DC105 and EIS300 software. A three-electrode cell equipped with a Pt counter-electrode, a Ag/AgCl/Cl⁻ (3-M KCl) reference electrode, and a coated or noncoated 2024-T3 AA panel with an exposed area of 0.36 cm^2 as the working electrode was used. All measurements were conducted in dilute Harrison's solution (0.35 wt % $(NH_4)_2SO_4$ and 0.05 wt % NaCl) at 25 ± 1 °C. This mixture of electrolytes is considered to emulate closely the atmospheric environment for aircraft [31]. Coatings were immersed in dilute Harrison's solution 15 min. prior to the test. The reported values of potentials shown in the polarization curves and listed in the tables are given relative to the Ag/AgCl/Cl⁻ reference

electrode. PDS's were acquired in the region from −50 mV *vs.* E_{oc} (open circuit potential) to the pitting potential, E_{pit}, as determined using the criterion described by Kelly *et al.* [32], wherein pitting occurs by the time the anodic current density of the specimen reached $J_a = 3 \times 10^{-5}$ A/cm^2.

EIS tests were performed in triplicate on a Gamry PC3/300 potentiostat using a Gamry Corrosion Measurement System CMS100 and CMS300 software. Coatings were immersed in dilute Harrison's solution for 30 min. before data acquisition. The electrode arrangement is identical to the above-described PDS cell setup. EIS spectra were acquired in the frequency (*f*) range of 10 mHz to 10 kHz (10^{-2}–10^{+4} Hz) with 10 mV-applied alternating current (*vs.* E_{oc}). Standard coating-analysis criteria are as follows: Impedance values of $|Z| > 10^9$ Ω·cm^2 are indicative of coatings with excellent barrier properties. Coatings with $10^6 \leq |Z| \leq 10^9$ Ω·cm^2 are considered to be good coatings. Coatings with $|Z| < 10^6$ Ω·cm^2 are considered to be poor coatings [33].

The polarization resistance method, using Gamry software, was used to define corrosion potential, E_{corr}; corrosion resistance, R_{corr}, which is defined as the slope of the current density–potential curve at the corrosion potential; and corrosion current density, J_{corr}, which is defined as 20 mV/R_{corr}, as per *ASTM G3-89*. PDS, using Gamry software, was used to define E_{corr} and E_{pit}.

8. Solid-State Nuclear Magnetic Resonance Spectroscopy

Solid-state nuclear magnetic resonance (NMR) experiments were performed on a Chemagnetics CMX-II 300-MHz (7.06-T) spectrometer using a Chemagnetics 300VXP-208 double-resonance (H–X) probe for data collection. Resonance frequencies for ^{13}C and ^{1}H were 75.6 and 301.0 MHz, respectively. All peaks were referenced to an external tetramethylsilane standard. Magic-angle spinning (MAS) was carried out in 5-mm zirconia rotors, spinning at 6

kHz. NMR spectra were collected with a quasi-adiabatic cross-polarization (CP) pulse sequence [34] using a 1-s pulse delay, a 2-ms contact time, a 4-μs pulse width, and 10,000 scans.

C.   Results and Discussion

1.   Characteristics of Single-Layer LBL and Ormosil Coatings

The multilayer LBL-assembled/Ormosil coatings investigated during this study were composed of an inhibitor-doped LBL basecoat and an Ormosil topcoat. Figure 1 shows a schematic of this coating system. Figure 2 shows the structures of the polyelectrolytes and silanes used in this study.
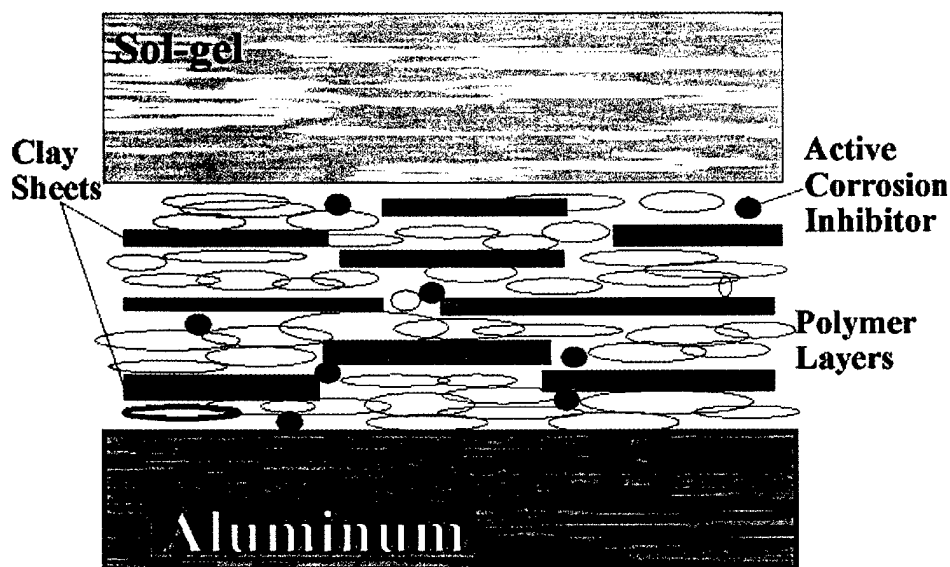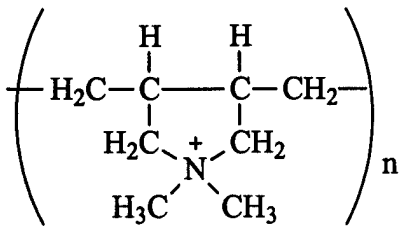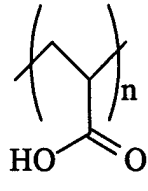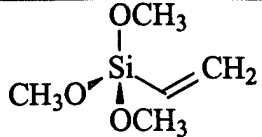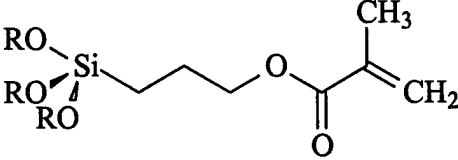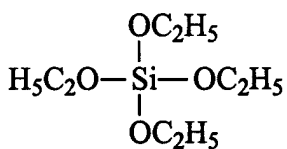

Figure 1: Representation of a Multilayer Coating System Comprising an Inhibitor-Doped LBL-Assembled Basecoat and a Sol–Gel-Derived Ormosil Topcoat

The LBL coating was prepared by the repetitive, sequential immersion of the substrate material in solutions of positively charged PDDA polycation, negatively charged PAA polyanion, and montmorillonite clay platelets in a fashion similar to that previously described by Kotov *et al*. [28]. Electrostatic attraction between the charged species produces thin, nanometer-scale monolayers on the substrate material.

Figure 2: Structures of Chemicals Used in this Study

LBL-assembled coatings containing different functionalities made from weak PE's can be used as reservoirs for ACI ions. Dilute aqueous dispersions of montmorillonite clay particles are known to exfoliate into single sheets (or thin platelets) in which the negative charge is balanced by inter- and intralamellar Na^+ cations. These montmorillonite sheets and platelets are expected to preferentially self-assemble parallel to the substrate [35] and to cover large surface areas, thereby smoothing defects introduced during the LBL film-formation process [36]. The negatively charged PAA may provide ion-exchange capacity for positively charged ions, such as Co^{3+} and Cr^{3+}. The positively charged PDDA may provide ion-exchange capacity for negatively charged ions, such as $Cr_2O_7^{2-}$. These characteristics are of interest to corrosion resistance studies due to (a) their ability to produce a dense, pore/defect-free layer; and (b) their capability of

allowing ion exchange with ACI ions. The presence of these exchange sites affords tremendous versatility and the possibility of fine-tuning the properties of LBL coatings for inhibitor absorption and corrosion protection.

The Ormosil coating investigated is a mixture of TEOS, VTMOS, and MEMO. Their $^1H-^{13}C$ CP/MAS NMR spectra, shown in Figure 3, indicate that the network structure of this Ormosil contains pendant vinyl and methacrylate groups that are expected to occupy pore space and surface positions. Distinct chemical shift peaks are observed in the $^1H-^{13}C$ CP/MAS NMR spectrum due to vinyl (138.3 and 130.1 ppm) and methacrylate (169.2, 137.7, 126.8, 67.1, 22.0, 18.2, and 8.5 ppm) functionalities [37]. Additional peaks are observed in the 0–35-ppm region, indicating small contributions from possible acid-catalyzed homopolymerization of vinyl groups. The presence of pendant groups is anticipated to make the Ormosil coating more hydrophobic, slowing the penetration of water and corrosion initiators.
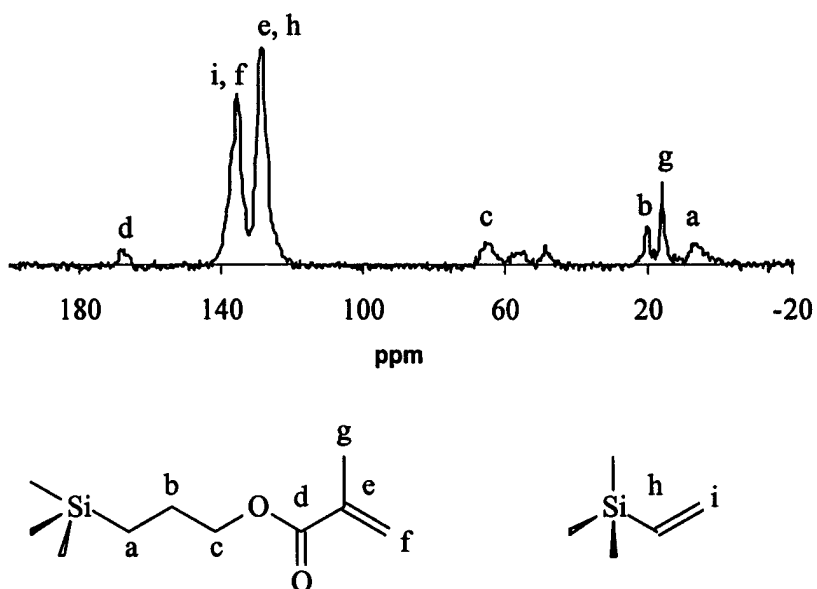

Figure 3: $^1H-^{13}C$ **CP/MAS NMR Spectra of a TEOS–VTMOS–MEMO Ormosil**

2. Characteristics of Inhibitors Investigated

Cr^{6+} and Co^{3+} ions were selected as inhibitors for this study based on their reported corrosion-resistance characteristics. Hexavalent chromium was chosen as a control because it is used as the active ingredient in standard military and industrial corrosion-resistance pretreatment for aluminum alloys. While the composition, structure, and mechanism of corrosion protection provided by chromate ions is not definitively known, extensive research in this area has provided insights into the unique aspects of these coating systems [38]. The cobalt conversion coating developed by Schriever was chosen based on the reported excellent corrosion-resistance characteristics, lower toxicity of cobalt(III) compared to chromium(VI), and reported good paint adhesion properties [1]. The cobalt conversion coating is prepared from an aqueous solution of a cobalt(II) salt, an ammonium salt, an inorganic complexing agent, an organic complexing agent, and an oxidizing agent, leading to the formation of highly stable cobalt(III) complexes that are stored in the oxide conversion coating. The complexes are believed to be of the general formula $Na_3[Co(NO_2)_2 \cdot (X)_4]$ (X = ^-OOCH, $^-OOCCH_3$, etc.) based on the reagents listed in the experimental portion of the patent. The soluble inhibitor complexes formed may migrate throughout the coating system and/or over the surface providing a self-healing repair process considered similar to that exhibited by the chromate conversion coating [1].

3. Coating Characterization Methods

Corrosion-resistance characteristics of single- and multilayer LBL/Ormosil coatings were analyzed using electrochemical techniques: polarization resistance method, potentiodynamic polarization scan, PDS, and EIS. Electrochemical analysis methods provide a quantitative description of coating characteristics.

The models used for coating analysis via EIS were the equivalent-electrical-circuit model for a simple-corroding-electrode model (*ASTM G3*) and the model for a typical coated metal, as

selected from the Gamry software. Figure 4 shows the equivalent circuits used to model the experimental data. Model (a) is a simple-corroding-electrode model (*ASTM G3*) used for analysis of bare AA's and Cr^{6+}/Cr^{3+}-treated metals, where R_u is the solution resistance; R_{pol} is the polarization resistance; R_{po} is the pore resistance; R_{tot} is the total resistance, the sum of the resistive components of the equivalent circuit, $R_{po} + R_{pol}$; and C_{dl} is the double-layer capacitance. Model (b) is typical of the coated metals used for LBL and Ormosil coatings, where C_c denotes the coating capacitance.

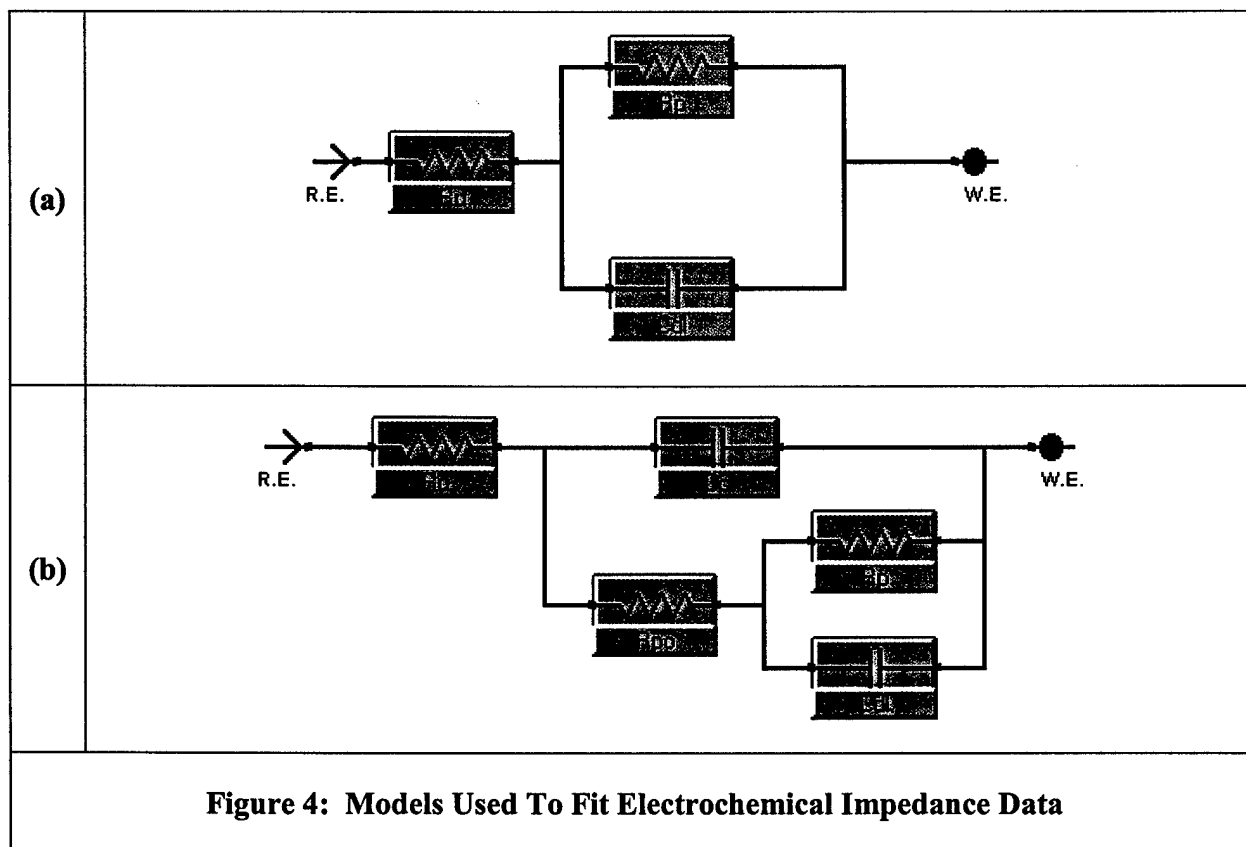**Figure 4: Models Used To Fit Electrochemical Impedance Data**

Figure 5 represents a typical Bode plot for a LBL film assembly (15 layers) on 2024-T3 AA, in which Curve 1 is a plot of $|Z(f)|$; Curve 2 is a plot of phase angle, $\varphi(f)$; and the solid line is a curve fit for a typical-coated-metal model. The undamaged coating generally exhibited very

high $|Z|$ values at low f. The approach of $\varphi \rightarrow -90°$ at low f is also indicative of a good, homogeneous coating.
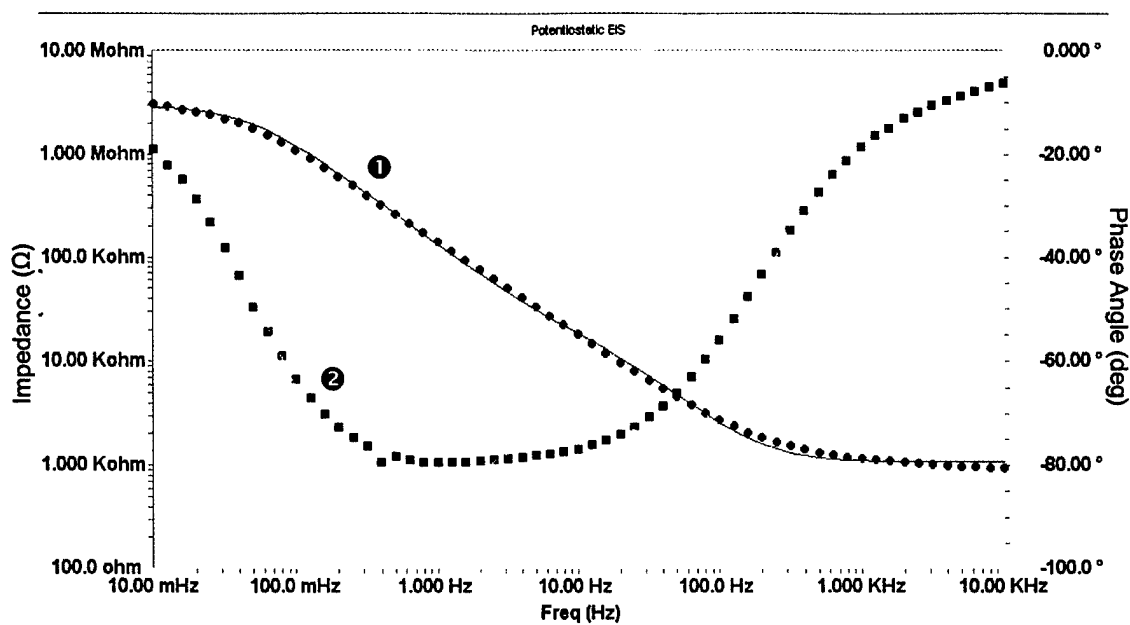

Figure 5: EIS Data Recorded for 15 Layers of LBL Coating

4. Corrosion-Resistance Characteristics of Inhibitors

Corrosion-resistance characteristics of Cr^{6+}- and Co^{3+}-based surface treatments were investigated using EIS and PDS. Table I and Table II present the numerical results while Figure 6 (p. 15) plots the PDS results for all coating systems investigated.

- Plot I displays values for (a) bare 2024-T3 AA, (b) AA treated with $K_2Cr_2O_7$, and (c) AA treated with a Co^{3+}-based conversion coating.

- Plot II displays values for (a) an LBL/Ormosil coating, (b) an Ormosil coating, and (c) an LBL coating ($n = 15$).

- Plot III displays values for (a) a Co-exchanged LBL coating and (b) a Cr-exchanged LBL coating.

- Plot IV displays values for (a) a Co-exchanged LBL/Ormosil coating system and (b) a Cr-exchanged LBL/Ormosil coating system.

**Table I: Electrochemical Characteristics Derived
from EIS for Coating Systems Under Investigation**

Composition	C_c, $\mu F/cm^2$	R_{pol}, $k\Omega \cdot cm^2$	R_{po}, $k\Omega \cdot cm^2$	R_{tot}, $k\Omega \cdot cm^2$	φ, deg
2024-T3 AA	—	48	—	48	—
0.25 M $K_2Cr_2O_7$	3	1580	10	1590	−64
Schriever	3	316	18	334	−47
LBL (n = 15)	2	1015	17	1032	−22
Ormosil	0.1	121	5	127	−12
LBL/Ormosil	0.2	1352	2	1355	−81
LBL+Co^{3+}	3	1922	8	1930	−63
LBL+Cr^{6+}	3	2520	15	2535	−80
LBL+Co^{3+}/Ormosil	8×10^{-3}	2038	137	2169	−62
LBL+Cr^{6+}/Ormosil	7×10^{-3}	2624	151	2775	−65

**Table II: Electrochemical Characteristics Derived
from PDS for Coating Systems Under Investigation**

Composition	$J_{corr} \times 10^7$, A/cm^2	E_{corr}, V	E_{pit}, V	R_{corr}, $k\Omega \cdot cm^2$
2024-T3 AA	5	−0.682	−0.509	49
0.25 M $K_2Cr_2O_7$	0.16	−0.390	−0.09	1500
Schriever	0.79	−0.348	−0.158	320
LBL (n = 15)	0.24	−0.477	−0.310	1042
Ormosil	1.95	−0.463	−0.02	128
LBL/Ormosil	0.19	−0.330	+0.11	1300
LBL+Co^{3+}	0.12	−0.410	−0.09	1985
LBL+Cr^{6+}	0.1	−0.390	+0.06	2500
LBL+Co^{3+}/Ormosil	0.09	−0.49	+1.3	2617
LBL+Cr^{6+}/Ormosil	0.12	−0.45	+0.88	2037

PDS data indicate the Cr^{6+} ion provides good corrosion-resistance characteristics, as R_{corr} was found to increase from 49 $k\Omega \cdot cm^2$ for bare AA to 1500 $k\Omega \cdot cm^2$ upon treatment with Cr^{6+} ions. Similarly, E_{corr} and E_{pit} values were found to shift to more-positive values from −0.682 V and −0.509 V for bare AA to −0.390 V and −0.09 V, respectively, for AA treated with Cr^{6+}. EIS data at low f also show the increase of R_{pol} from 48 $k\Omega \cdot cm^2$ to 1580 $k\Omega \cdot cm^2$ upon treatment with Cr^{6+} ions. The Co^{3+}-based conversion coating developed by Schriever showed a low R_{tot} value of 334 $k\Omega \cdot cm^2$. The values of E_{pit} and E_{corr} were shifted to −0.158 and −0.348 V, respectively, indicative of a coating providing some corrosion protection. As with the Cr^{6+} treatment, high C_c

values indicate the thin nature of this conversion coating, taking into consideration the inverse

relationships between coating capacity and film thickness.

Figure 6: Potentiodynamic Scans
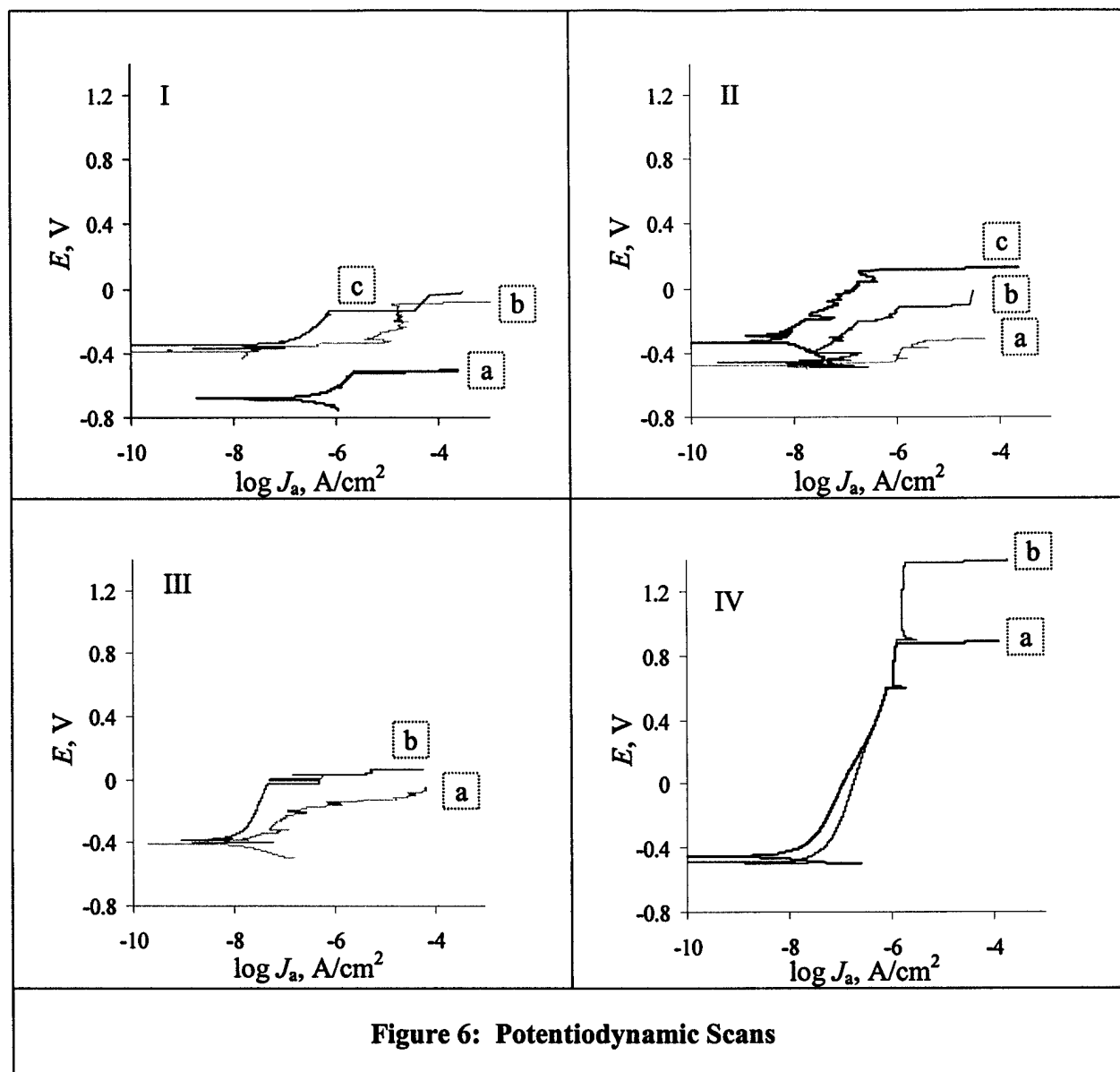
5.   Optimization of LBL Coating Properties

In order to determine the optimum number of polyelectrolyte layers needed for complete

AA-substrate-surface coverage, electrochemical characteristics were investigated as a function of

the number of layer deposition cycles, as reported in Table III.

Table III: Electrochemical Characteristics for LBL Coatings on 2024-T3 Aluminum Alloy as a Function of the Number of LBL Films Deposited

n	C_c, µF/cm^2	R_{po}, kΩ·cm^2	R_{pol}, kΩ·cm^2	R_{tot}, kΩ·cm^2
2024-T3 AA	—	—	42	42
3	4.1	8	374	384
5	4.1	6	396	402
7	4.7	12	344	356
9	5.3	11	540	551
11	3.7	11	544	555
13	5.3	14	1361	1375
15	1.9	17	1015	1032
17	1.0	21	1404	1329
20	1.0	17	1010	1027

Figure 7 plots $R_{tot}(n)$ values. As n increased from 0 to 5, an increase in R_{tot} from 42 to 402 kΩ·cm^2 was observed. An increase in n from 5 to 11 did not significantly increase the value of R_{tot}. An increase in n from 11 to 13 led to a further increase in R_{tot} from 555 to 1375 kΩ·cm^2. When the number of polyelectrolyte layers increased to $n = 20$, it did not appear to increase R_{tot}. For coatings prepared from $n = 20$, a dramatic *decrease* in film adhesion was observed, as these coatings were found to readily delaminate from the substrate. For this reason, $n = 15$ was chosen
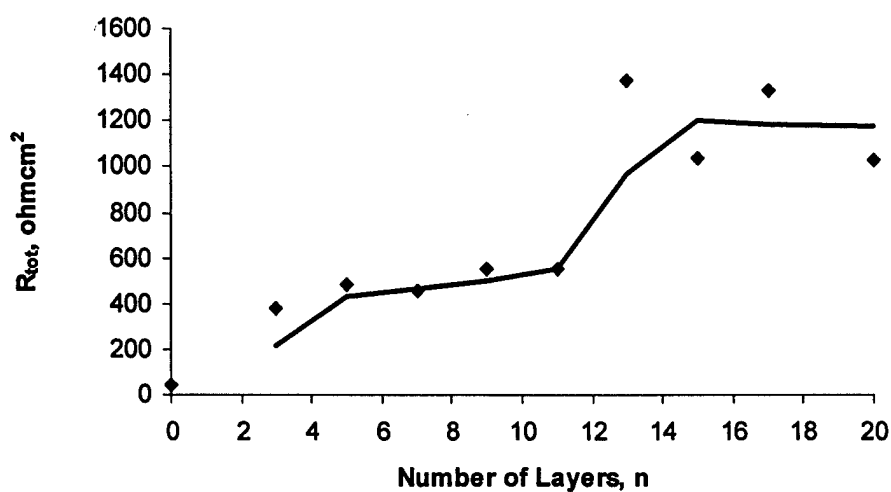

Figure 7: Total Resistance as a Function of the Number of Layers

as the optimum LBL coating for further investigation, as this coating thickness appears to provide good AA surface coverage and to maintain good adhesion characteristics.

A decrease is observed in C_c extracted from the typical-coated-metal model from 5.3 μF/cm^2 for $n = 9$ PE layers to 1.9 μF/cm^2 for $n = 15$

$$(1) \quad C_c = \frac{\varepsilon_r \varepsilon_0 A}{d}$$

and further to 1.0 μF/cm^2 for $n = 20$. Considering Equation (1), which defines C_c in terms of ε_r, the relative dielectric constant; ε_0, the absolute dielectric constant of a vacuum (8.85 $\times$ 10^{-12} F/m); A, the electrode surface area; and d, the coating thickness, this behavior is indicative of an increase in d of the LBL assembly [39]. It is anticipated that the addition of each subsequent LBL-assembled layer would lead to a gradual linear increase in d and therefore in R_{tot}. However, this behavior is *not* observed. Two regions were observed in which R_{tot} remained relatively constant with increasing n. This behavior may be attributed to the AA surface preparation and/or homogeneity. In the event that the AA substrate contains islands that are not charged or are hydrophobic due to insufficient cleaning, inhomogeneous coating deposition would be observed. During the first few layers, a nonlinear increase in coverage is observed as the film is covering properly cleaned areas in preference to defect sites. With repetition of the film-deposition procedure, the surface becomes covered, leading to real film growth and an increase in R_{tot}. Until the first complete layer is deposited, C_c is determined by the AA surface inhomogeneities.

Despite increases in R_{tot} with n, a significant increase in corrosion resistance was *not* observed upon coating the AA with the $n = 15$ LBL film. R_{corr} values were found to be 1042 k$\Omega \cdot$cm^2 compared to 1500 k$\Omega \cdot$cm^2 for Cr^{6+}-based coating. Observed E_{corr} values were found to be -0.682, -0.390, and -0.477 V for bare AA, Cr^{6+}-treated AA, and a $n = 15$ LBL-assembled coating, respectively. Similarly, E_{pit} values were -0.509, -0.09, and -0.310 V for analogous coatings. This shift into the more-positive potential region for E_{corr} and E_{pit} indicates the

formation of a thin, protective film on the substrate; while the LBL film assembly may provide minimal corrosion protection, the corrosion-resistance performance of the Cr^{6+} is superior to that of the LBL film assembly. The φ for $|Z|$ at low f is closer to $-90°$ for Cr^{6+} ($-64°$) than for a $n = 15$ LBL coating ($-22°$), also indicative of the superior coverage and corrosion-protection properties of Cr^{6+}. Despite the low corrosion-protective properties afforded by the LBL coating, R_{po} was found to be in the range of $6–21$ $k\Omega \cdot cm^2$ for all investigated systems; these results indicate that the LBL coating forms a passivating layer on the surface of the Al_2O_3 and increases the natural Al_2O_3 resistance.

6.   Corrosion Protection Provided by Incorporation of Montmorillonite Clay Platelets

Recent work by Dai has shown that alternating PE thin films without clay particles inside the layer structure provides good corrosion protection for aluminum surfaces [40]. To determine the corrosion-protective properties of the montmorillonite clay platelets in the LBL assembly, PDDA/PAA/clay LBL assemblies were compared to analogous PDDA/PAA coatings prepared without clay particles in the layer structure. Table IV shows results of electrochemical analysis for these coating systems. Impedance data indicate that incorporation of clay platelets increases R_{pol} for $n = 13$, 15, and 17 coatings by more than twofold. The R_{pol} values are in the ranges of $447–501$ and $1010–1404$ $k\Omega \cdot cm^2$ for $n = 13–17$ coatings without and with the clay platelets, respectively. The R_{po} is very small for both systems, but the value for PDDA/PAA assemblies is one order of magnitude lower than for PDDA/PAA clay assemblies. The C_c is more than two times lower for $n = 13–17$ layered films containing clay platelets than for analogous coatings prepared without clay platelets; this behavior may be indicative of their increased thickness and better protective properties, as surface passivation generally increases with coating thickness.

**Table IV: Electrochemical Characteristics for LBL Coatings
With and Without Clay Platelets on 2024-T3 Aluminum Alloy**

n	Composition	C_c, $\mu F/cm^2$	R_{po}, $k\Omega \cdot cm^2$	R_{pol}, $k\Omega \cdot cm^2$	R_{tot}, $k\Omega \cdot cm^2$
13	PDDA/PAA	4.4	1	501	502
15	PDDA/PAA	5.0	1	447	448
17	PDDA/PAA	5.0	1	502	503
13	PDDA/PAA/Clay	5.3	14	1361	1375
15	PDDA/PAA/Clay	1.9	17	1015	1032
17	PDDA/PAA/Clay	1.0	21	1404	1329

These data indicate that clay platelets provide the LBL films with additional corrosion-protective properties. In the course of LBL deposition they are assembled into well-ordered structures wherein individual sheets are oriented parallel to each other and to the substrate surface. Platelet organization of this type yields a very high barrier function, approximately 12× higher than in the case of PE combinations with random platelet orientations. LBL organization greatly reduces the permeation of gases and ions through such films [41].

7. Corrosion-Resistance Characteristics of the Ormosil Thin Film

The Ormosil used in this study provided moderate corrosion-resistance characteristics for the 2024-T3 AA substrate. R_{corr} was 128 k$\Omega \cdot cm^2$; similarly, R_{po} was low, 5 k$\Omega \cdot cm^2$, indicative of porosity present in the coating. C_c was smaller for the Ormosil coating than for the LBL coating, indicating that the thickness of the Ormosil was greater than that of the LBL coating (assuming that that they have similar ε_r values). E_{corr} and E_{pit} were found to shift in the positive direction upon coating the metal substrate with the Ormosil coating. For example, E_{corr} was found to increase from −0.682 to −0.463 V and E_{pit} was found to increase from −0.509 to −0.02 V, indicating an enhancement in corrosion protection afforded by coating the AA surface with the Ormosil thin film. The moderate corrosion protection afforded by the Ormosil coating was confirmed by the salt-spray test (results not shown), as localized pitting was observed on the test coupon. Corrosion-resistance properties of the Ormosil coating may be attributed to moderate

barrier properties and to excellent compatibility and adhesion between the metal substrate and the Ormosil coating.

8.   Corrosion-Resistance Characteristics of Inhibitor-Doped LBL Films

Introduction of known ACI ions using the exchange capacity of the LBL coating gives an increase of corrosion-resistance characteristics of the LBL films. Inhibitor incorporation was not found to change d significantly, as C_c remained in the same range for non-doped and inhibitor-doped LBL film assemblies. R_{tot} was found to increase from 1032 $k\Omega{\cdot}cm^2$ for non-doped LBL to 1930 and 2535 $k\Omega{\cdot}cm^2$ for Co^{3+}- and Cr^{6+}-doped LBL films, respectively. Similarly, E_{corr} values were found to increase slightly from −0.477 V for non-doped LBL to −0.410 and −0.390 V, for Co^{3+}- and Cr^{6+}-doped LBL films, respectively; E_{pit} values were also found to increase from −0.310 V for non-doped LBL to −0.09 and +0.06 V, for Co^{3+}- and Cr^{6+}-doped LBL films, respectively. Analogously, φ also changed from −22° to −63° and −80° for Co^{3+}- and Cr^{6+}-exchanged LBL coatings, respectively.

9.   Multilayer Coating Systems

Figure 8 shows a scanning electron micrograph (SEM) of the cross-section of an LBL/Ormosil coating system. Five distinct regions are observed in this image: (1) the AA substrate, (2) the LBL coating, (3) the LBL coating/sol–gel coating interfacial layer, (4) the sol–gel coating, and (5) the imbedding polymer matrix. From this image, the LBL, interface, and sol–gel coating thicknesses are estimated to be approximately 0.5, 0.5, and 1 µm, respectively.

Although ACI ions are expected to retain some of their mobility in the LBL/Ormosil coating system, the ACI ions are anticipated to be concentrated in the LBL coating. The uppermost portion of the LBL coating may become sealed by the sol–gel film as curing may promote condensation reactions between the sol–gel film and the clay platelets, resulting in a

thin interfacial layer. The LBL coating near the AA surface is expected to remain unchanged
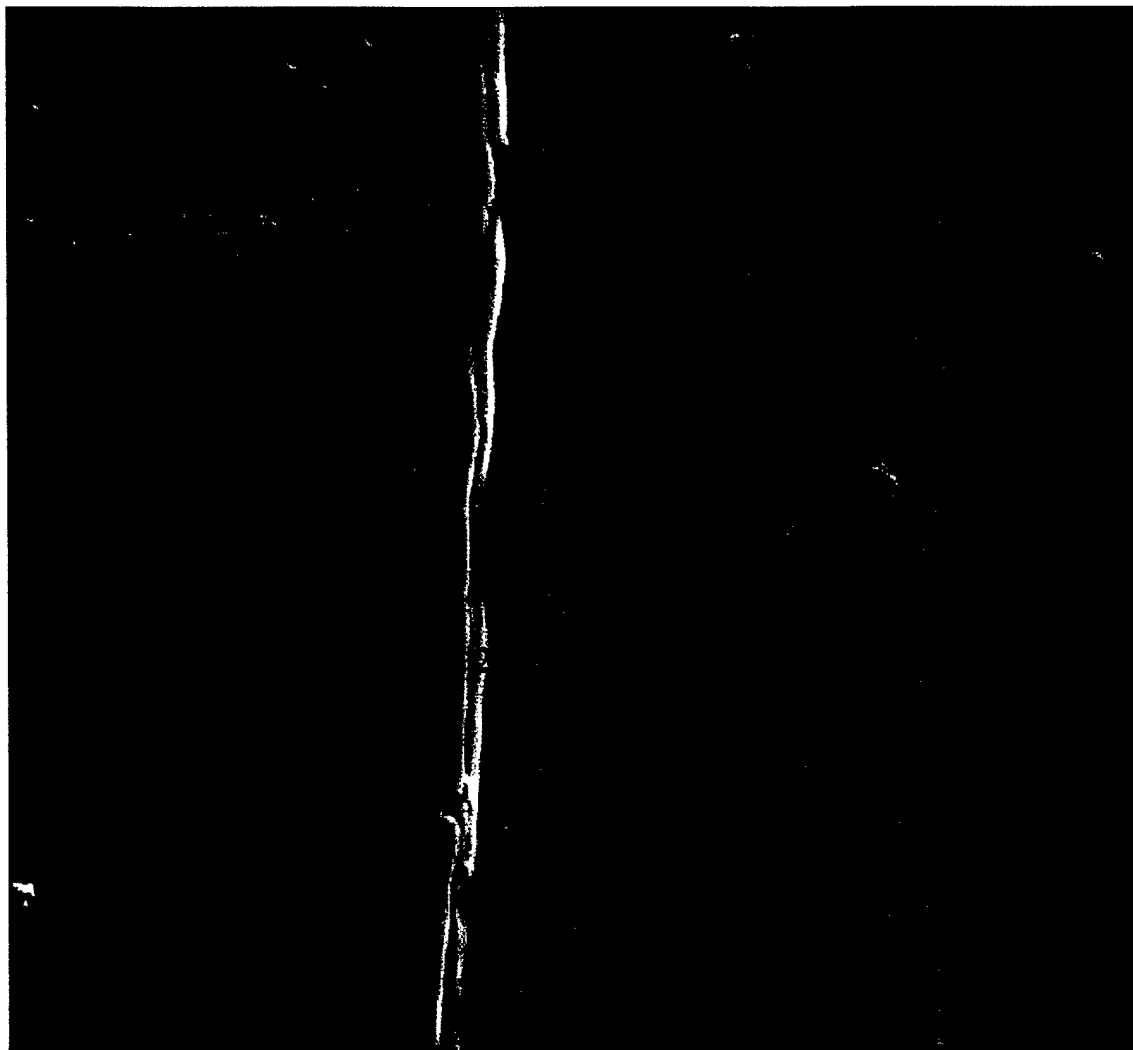
and to serve as a medium for ACI diffusion.

Figure 8: Cross-Section of an LBL/Ormosil Coating System (SEM)

10. Non-Inhibitor-Doped LBL/Ormosil

Additional corrosion protection is provided when the LBL coating is used in combination

with the sol–gel coating when compared to the LBL or Ormosil coatings alone. R_{tot} was found to

increase from 1032 kΩ·cm^2 for non-doped LBL to 1355 kΩ·cm^2 LBL/Ormosil multilayer films.

E_{corr} values increased from −0.477 V for LBL to −0.330 V for the LBL/Ormosil coating; E_{pit}

values were also found to increase from −0.310 V for non-doped LBL to +0.11 V for

LBL/Ormosil multilayer coatings. The φ at low f for the 15-layer LBL film/Ormosil is $-81°$, indicative of a good quality, undamaged coating. These properties also indicate that the Ormosil layer is highly compatible with the underlying LBL coating.

11. Inhibitor-Doped LBL/Ormosil Multilayer Coating Systems

Combination of an inhibitor-doped LBL coating with an Ormosil coating was found to enhance the corrosion-resistance characteristics of the LBL coatings. R_{tot} was found to increase from 1355 kΩ·cm^2 for LBL/Ormosil to 2169 and 2775 kΩ·cm^2 for Co^{3+}- and Cr^{6+}-doped LBL/Ormosil films, respectively. For these coating systems, E_{corr} values were found to decrease from -0.330 V for non-doped LBL to -0.49 and -0.45 V, for Co^{3+}- and Cr^{6+}-doped LBL/Ormosil films, respectively; E_{pit} values were found to dramatically increase from $+0.11$ V for non-doped LBL to $+1.3$ and $+0.88$ V for Co^{3+}- and Cr^{6+}-doped LBL films, respectively. R_{po} increased from ≤ 15 kΩ·cm^2 for all other LBL/Ormosil combinations to 137–151 kΩ·cm^2, indicating the combination of the Ormosil barrier properties with those of the inhibitor-doped LBL coating produces a coating system in which it is harder to penetrate the pores.

12. Performance Characteristics of Multilayer LBL/Ormosil Coating Systems

Ion-exchanged LBL/Ormosil coatings were found to provide good corrosion protection of 2024-T3 AA. Synergistic properties of the component layers are expected to contribute to the corrosion-resistance properties. The coating system is composed of (a) an inhibitor-doped LBL base layer and (b) a dense, sol–gel-derived topcoat, as shown in Figure 9. The inhibitor-doped LBL coating is expected to provide a reservoir for ACI ions. In the absence of reactions leading to corrosion, the ions are immobilized within the LBL coating due to electrostatic attractions between the ion and the charged polyelectrolyte or clay layers. The dense sol–gel-derived topcoat provides a primary mechanism of barrier corrosion protection.
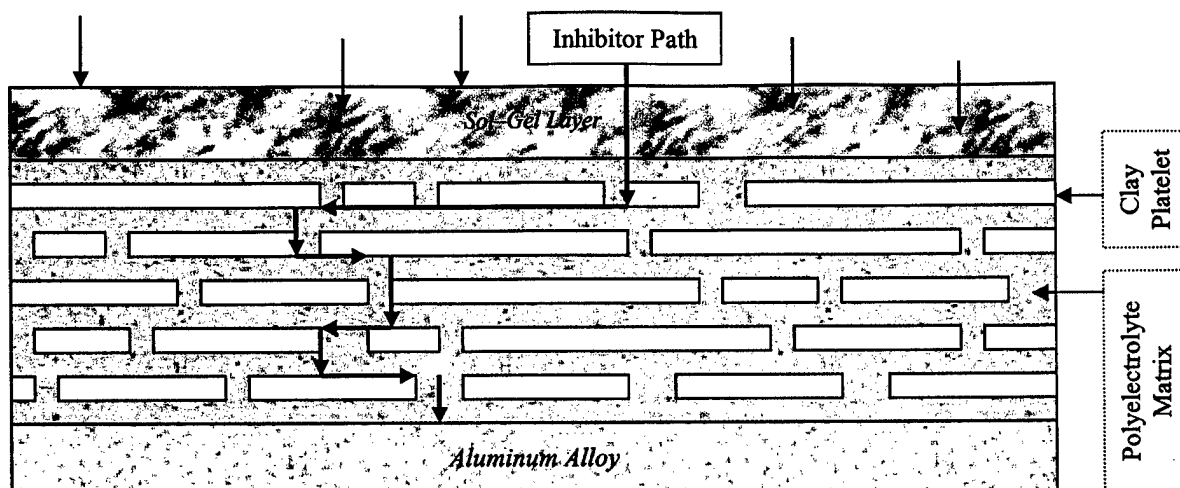
Figure 9: Representation of the Migration of Active Corrosion Inhibitor Ions through the Multilayer LBL/Ormosil System

In the event that the integrity of the sol–gel layer is breached, water and other corrosion initiators may permeate into the LBL coating, promoting migration of ions within it. The permeation rates of H_2O, O_2, and ACI's are expected to decrease as a function of (a) LBL coating thickness, density, and defect content; (b) Ormosil coating thickness, density, and pore size; (c) overall coating system density and adhesion to metal substrate; and (d) compatibility between the LBL and sol–gel coatings.

T_r-cured Ormosil thin films are expected to contain a certain amount of inherent porosity, dependent on cure time and the catalyst used. The acid catalysis used in this study may produce linear siloxane chains that yield a higher-density coating than those prepared using base catalysis. However, the presence of open, interconnected porosity in the Ormosil thin film is expected to provide channels for the migration of corrosion initiators through the coating, even though the rate of penetration should be slowed significantly.

In ACI-doped LBL films, the corrosion initiators that penetrate the sol–gel coating are expected to be attracted to the ion-exchange capacity of the montmorillonite clay platelets. The presence of small amounts of water are expected to aid in the migration of these species along

the clay platelets, parallel to the AA surface, thereby providing a more difficult path for the initiators to follow towards the metal as compared to a straight channel or open pore. The initiators potentially may also be absorbed by the clay platelets, limiting their migration.

D.   Conclusions

Single- and multilayer LBL/Ormosil coating systems were investigated. The optimum number of layers for the LBL coating was found to be $n = 15$, as this thickness provided adequate substrate coverage and adhesion. Although the resistance of LBL coatings is minimal, they form the passivating layer on the surface aluminum oxide and increase the oxide resistance. Incorporation of ACI's was found to increase the corrosion resistance of the LBL coatings. The application of a dense barrier Ormosil layer was found to seal the ACI's into the LBL coating, providing a reservoir of ACI's. The LBL/Ormosil coating system provides several functions, including: (a) the barrier properties of the Ormosil layer result in a reduction of the concentration of corrosion initiators that come in contact with the ACI reservoir and ultimately the metal substrate; (b) the LBL coating may potentially change the pathway/rate by which the initiators approach/migrate to the AA; and (c) the exchanged LBL coating may release ACI ions in the vicinity of a defect site, thereby mitigating corrosion reactions on the metal surface.

II.   Release-on-Command Technologies

A.   Introduction

LBL/Ormosil coating systems on AA's provide an interesting challenge for coating removal. This behavior stems from the fact that these coating systems *are not susceptible to degradation* using common techniques employed for the removal of organic coatings from metal substrates, presumably due to the potential to form covalent Si–O–Al bonds with the underlying Al_2O_3 surface layer and their chemical inertness. The main goal of this portion of the research effort was to determine a coating-removal technique that will remove both Ormosil and LBL

coatings "on demand" without destroying the AA surface. Two coating removal methodologies were investigated: (a) immersion in a basic zincate solution and (b) immersion in a dilute sodium oxalate solution.
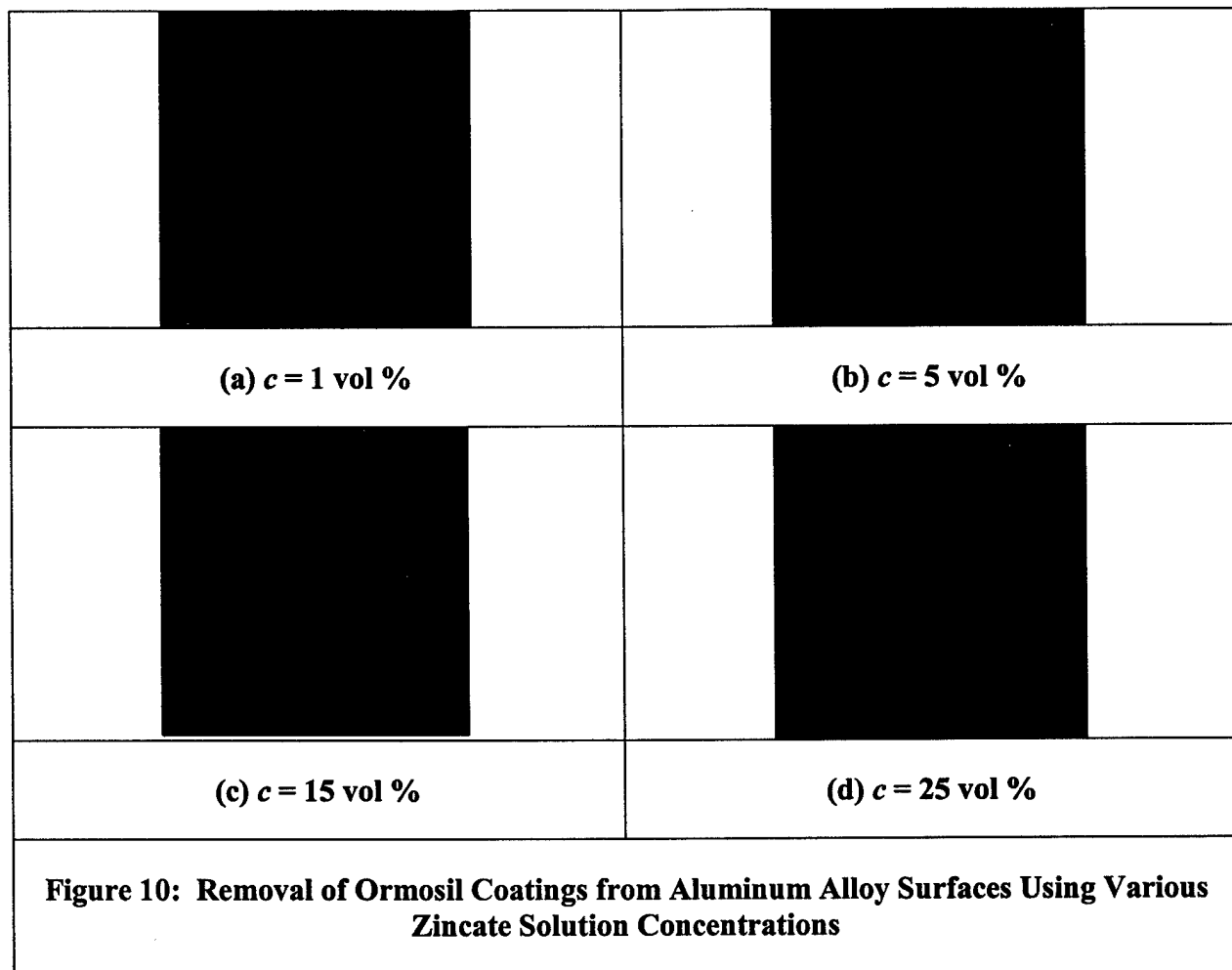
B. Ormosil Dissolution in Various Solvents

Various acidic, basic, and organic solvents were investigated as Ormosil-coating-removal agents from 2024-T3 AA substrates. Table V shows the results of 30-min. immersion experiments. Polar organic solvents, such as alcohols and ketones, were found to affect the Ormosil coatings investigated. The effectiveness of the alcohol was found to be inversely proportional to the

Table V: Effects of Various Solvents on the Ormosil Coatings Under Investigation

Solvent	Coating Condition
Methanol	Flaked Off
Ethanol	Not Affected
Isopropanol	Not Affected
Acetone	Flaked Off
Methyl Ethyl Ketone	Flaked Off
Hexanes	Not Affected
5-M HNO_3	Cracked
5-M $HC_2H_3O_2$	Not Affected
5-M H_2SO_4	Not Affected
5-M H_3PO_4	Not Affected
5-M NH_4OH	Flaked Off
5-M NaOH	Removed

length of the hydrocarbon chain, as methanol was found to affect the Ormosil, while ethanol and isopropanol were not. It is anticipated that the effectiveness of alcohol- and ketone-based solvents resides in the ability of these solvents to solubilize the organic portions of the Ormosil coating, thereby degrading the integrity of the coating. Hexanes solution, a nonpolar organic solvent, was not found to affect the integrity of any of the Ormosil coatings. Acidic solutions, prepared from either strong or weak acids, were not found to remove the Ormosil coating, though HNO_3 was found to cause cracking. Basic solutions were found to degrade the Ormosil coating. For example, 5-M NH_4OH promoted Ormosil film flaking as the coating dried after the immersion period; 5-M NaOH was found to remove effectively each of the four investigated Ormosil coatings from the AA substrate. While basic solutions were shown to be effective for

removing the Ormosil coating from the AA substrate, these reagents may potentially attack the

AA substrate, leading to degradation of the metal.

(a) $c = 1$ vol %	(b) $c = 5$ vol %
(c) $c = 15$ vol %	(d) $c = 25$ vol %

Figure 10: Removal of Ormosil Coatings from Aluminum Alloy Surfaces Using Various Zincate Solution Concentrations

In order to avoid degradation of the metal substrate, zincate solutions were also

investigated as potential coating-removal reagents. Zincate is a highly basic solution containing

zinc compounds commonly used in electroless and electroplating applications. In this study,

zincate solutions were found to remove the Ormosil coating from the AA effectively, leaving a

thin zincate layer on the AA surface. This is illustrated in Figure 10, in which the dark area

represents a thin zinc layer on the AA. Very low zincate concentrations, $c \leq 1$ vol %, were found

to be ineffective for removing the Ormosil coatings from the AA substrate. Increasing the

zincate concentration to $c \approx 5$ vol % facilitated coating removal. Higher zincate concentrations, $10 \leq c \leq 25$ vol %, were found to be highly effective for coating removal.

C.   LBL/Ormosil Coating Removal Using Dilute Zincate Solutions

Figure 11 shows that coating removal time (t_{cr}) was found to depend on the zincate concentration. For the investigated Ormosil film, increasing c to 15 vol % led to a decrease in t_{cr}. For the Ormosil coating under investigation, increasing the zincate solution to higher c produced a slight increase in t_{cr}. The t_{cr} value is also expected to be a function of coating composition and structure, as thicker coatings may require a longer immersion time (t_i).
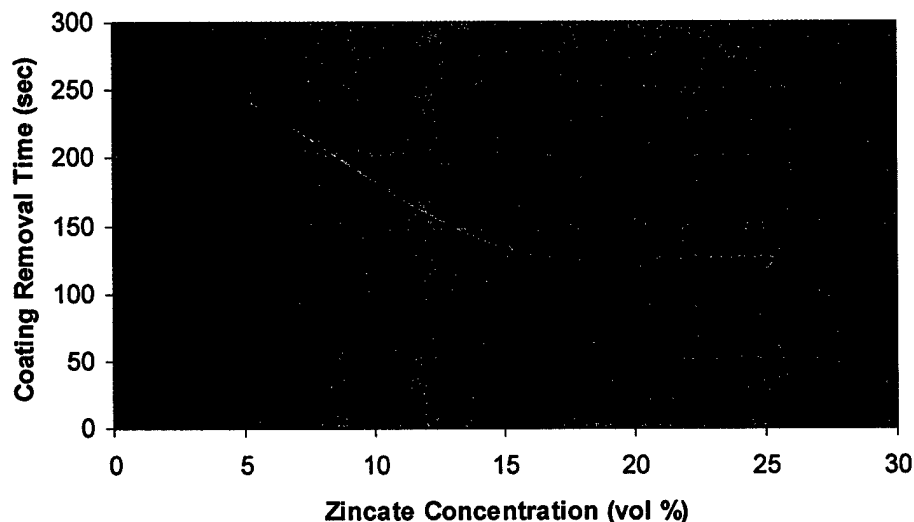

Figure 11: Coating Removal Behavior as a Function of Zincate Concentration for an Ormosil Coating

In order to produce a clean AA substrate, the residual zinc layer was easily removed using a dilute phosphoric acid solution. For this purpose, very dilute solutions, $c(H_3PO_4) \leq 2$ vol %, were the most effective for zinc removal. Higher H_3PO_4 concentrations were found to be ineffective for removing the zinc layer. The results of this study indicate that a combination of coating removal using the zincate solution followed by zinc removal using dilute phosphoric acid

effectively removes the Ormosil coating and restores the AA surface; at this point, the cleaned AA is prepared for additional coating application as needed.

In summary, dilute zincate solutions may be used to remove effectively Ormosil coatings from 2024-T3 AA's at T_r. The coating removal technique leaves a thin layer of zinc on the AA surface, which prevents further attack of the metal surface by the basic zincate solution. The zinc layer may be removed easily by immersion in dilute H_3PO_4, which maintains the integrity of the AA surface.

D.   LBL Coating Dissolution

1.   Zincate Solution

LBL film assemblies, taking into consideration their main components, also provide an interesting challenge for coating removal. Experiments show that dissolution of LBL coating assemblies from the AA surface using dilute alkaline zincate solution requires more-concentrated solutions than removal of the Ormosil thin films does, as is shown in Figure 12. (As in Figure 10, the dark area represents a thin zinc layer on the AA.) These results indicate that only a 25-vol-% zincate solution can effectively remove the LBL coating assembly from the AA surface, compared with complete removal of investigated Ormosil thin films starting with 5 vol %.

Optimization of the coating-removal conditions for the LBL/Ormosil coating system indicates that a 25-vol-% zincate solution will remove both coatings in 3 min., as is shown in Figure 13. The dark area represents a thin zincate layer on the AA; coating removal using zincate solution leaves a thin layer of zincate product on the AA surface. Subsequent zincate product removal using dilute H_3PO_4 restores the AA surface.

(a) Bare AA	**(b) LBL, *n* = 15**	**(c) *c* = 2.5 vol %**
(d) *c* = 5 vol %	**(e) *c* = 15 vol %**	**(f) *c* = 25 vol %**

Figure 12: Removal of LBL Coatings from Aluminum Alloy Surfaces Using Various Zincate Solution Concentrations
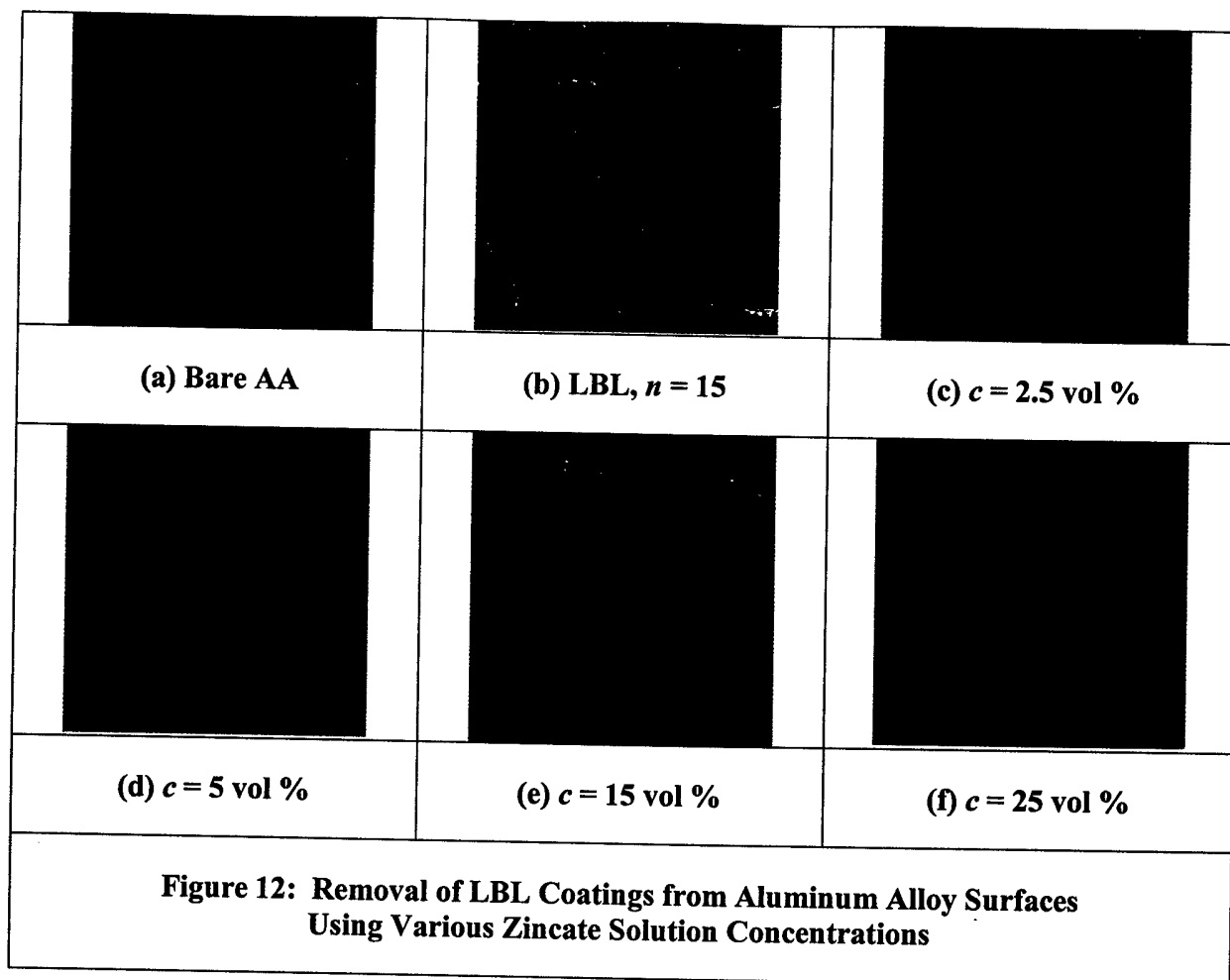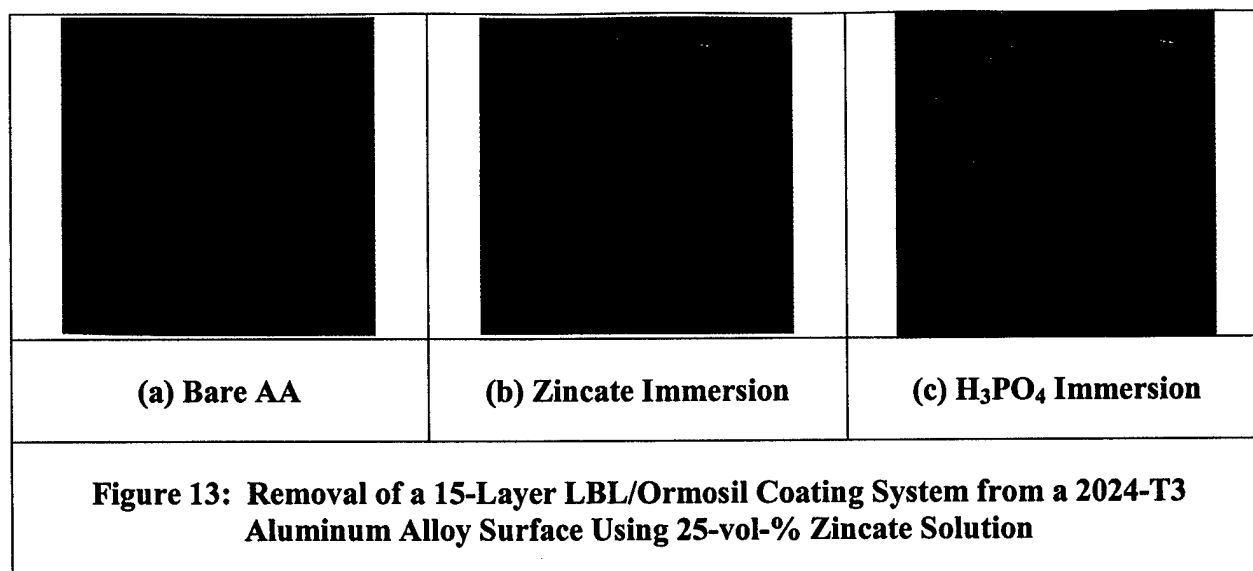
Figure 13(a) shows bare AA after a 4-min. immersion in 2% H_3PO_4 as a comparison. Figure 13(b) shows the partial removal of a 15-layer LBL/Ormosil coating (top) following a 3-min. immersion in 25-vol-% zincate (bottom). Figure 13(c) shows the partial removal of the same 15-layer LBL/Ormosil coating (top) following a 3-min. immersion in 25-vol-% zincate (middle), followed in turn by a 4-min. immersion in 2-vol-% H_3PO_4 (bottom). As was the case for the Ormosil coating, in order to produce a clean AA substrate, the residual zincate layer was easily removed using a dilute H_3PO_4 solution.

| (a) Bare AA | (b) Zincate Immersion | (c) H₃PO₄ Immersion |

Figure 13: Removal of a 15-Layer LBL/Ormosil Coating System from a 2024-T3 Aluminum Alloy Surface Using 25-vol-% Zincate Solution

2. Coating Removal Using Oxalate Solutions

An alternative coating-removal method for LBL coatings was to use dilute sodium oxalate solutions. $Na_2C_2O_4$ was chosen based on its known ability to passivate aluminum surfaces [42] and to form chelate complexes with the aluminosilicate portion of the clay particles that make up an integral part of the LBL composition.

Removal of the LBL coating system and the subsequent loss of corrosion-protective properties it provided were monitored using EIS. Electrochemical analysis indicated a decrease in R_{tot} of the investigated coating system during the incubation in $Na_2C_2O_4$ solution is dependent on c and pH, as is shown in Table VI. R_{tot} was found to decrease during the incubation in the $Na_2C_2O_4$ solution as a function of time for each of the three concentrations of $Na_2C_2O_4$ investigated, as is shown in Figure 14. From this data it is inferred that the more concentrated $Na_2C_2O_4$ solution ($c = 10^{-3}$–10^{-2} M, pH = 6.8) the steeper the slope of the polarization resistance *vs.* time curve. These results indicate that t_{cr} is inversely proportional to $c(Na_2C_2O_4)$.

Table VI: EIS Characteristics as a Function of LBL Coating Removal Time in Various Sodium Oxalate Solutions

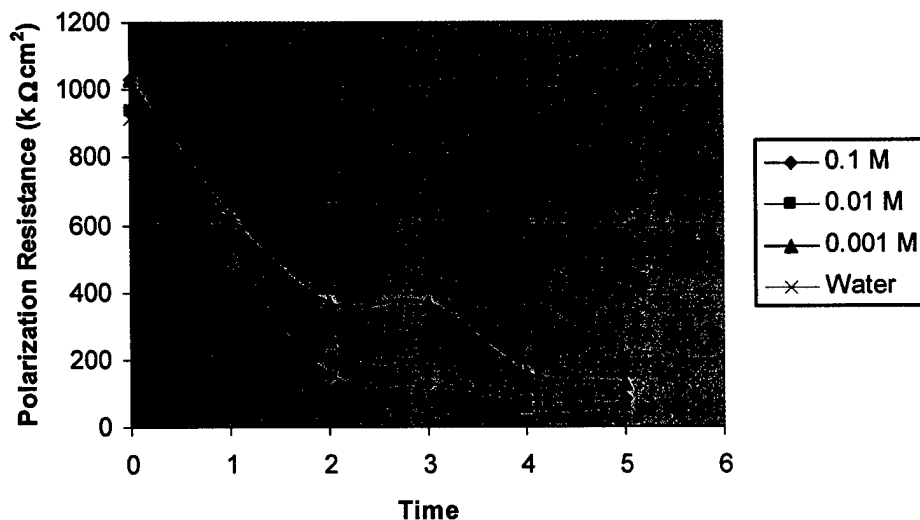| $c(C_2O_4^{2-})$, M	pH	t_b h	C_c, μF/cm^2	R_{pob} kΩ·cm^2	R_{po}, kΩ·cm^2	R_{tot}, kΩ·cm^2
—	—	0 (2024-T3 AA, freshly deoxidized)	—	2	—	2
—	—	0 (bare AA with natural oxide layer)	—	48	—	48
—	—	0 (n = 15 LBL)	1.9	1015	17	1032
10^{-1}	6.8	1	3.5	569	23	592
10^{-1}	6.8	2	7.8	115	40	155
10^{-1}	6.8	3	6.3	119	11	130
10^{-1}	6.8	4	5.3	81	3	84
10^{-1}	6.8	5	5	79	1	80
10^{-2}	6.8	1	2.0	487	11	498
10^{-2}	6.8	2	6.2	241	43	244
10^{-2}	6.8	3	6.0	127	32	159
10^{-2}	6.8	4	4.8	46	9	55
10^{-2}	6.8	5	4.9	47	9	56
10^{-3}	6.8	1	1.9	615	10	625
10^{-3}	6.8	2	1.2	331	37	368
10^{-3}	6.8	3	1.2	316	53	369
10^{-3}	6.8	4	5.2	136	23	159
10^{-3}	6.8	5	5.0	112	18	130
10^{-2}	10.3	0 (n = 15 LBL)	1	883	17	900
10^{-2}	10.3	1	8	90	17	107
10^{-2}	10.3	2	7	59	11	70
10^{-2}	10.3	3	44	32	2	34
10^{-2}	10.3	4	46	31	2	33
10^{-2}	10.3	5	47	32	2	33

Figure 14: Total Polarization Resistance During the Incubation in Various Sodium Oxalate Solutions as a Function of Solution Concentration and Time

Increasing the pH of the 0.01-M $Na_2C_2O_4$ solution from 6.8 to 10.3 of 0.01 M was found to facilitate LBL coating removal from AA specimens, as is plotted in Figure 15 and illustrated in Figure 16. For all investigated $Na_2C_2O_4$ solutions (10^{-3}–10^{-1} M, pH = 6.8), R_{tot} of immersed LBL-coated AA specimens (15 layers) was not reduced to $\leq$48 kΩ·cm^2, the total polarization resistance of AA with natural oxide film on its surface. This is indicative of the benign effect $Na_2C_2O_4$ has on the Al_2O_3 surface during the incubation period and indicates that residual $C_2O_4^{2-}$ ions on the AA surface provide an inhibitive effect after the LBL coating systems have been removed. $Na_2C_2O_4$ solutions were found to remove the LBL coating system and to provide corrosion protection for the underlying metal.
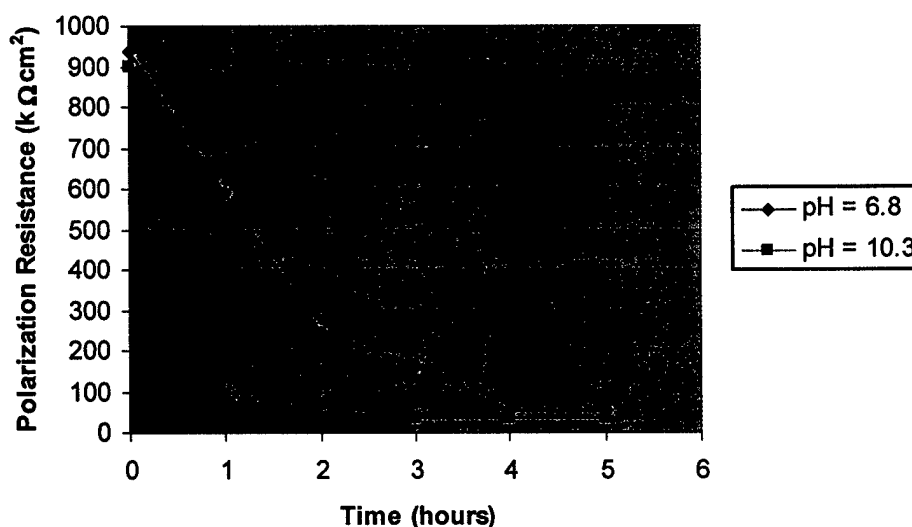

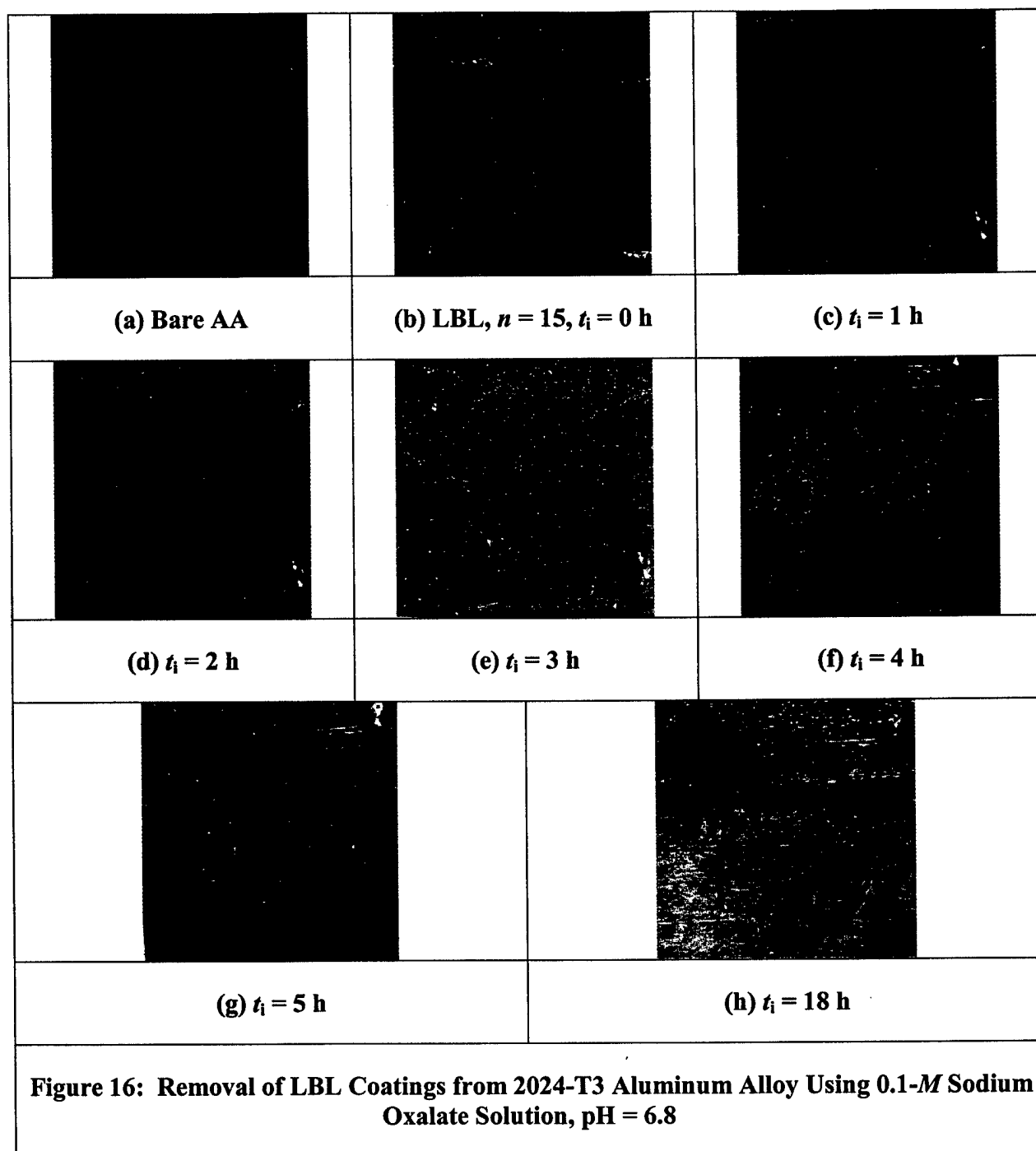**Figure 15: Total Polarization Resistance During the Incubation in 0.01-M Sodium Oxalate Solution as a Function of pH and Time**

E.   Summary

In summary, two methods were investigated by which to remove the LBL/Ormosil coating systems from the AA substrate "on demand." Zincate solutions were found to be effective for the rapid removal of the LBL/Ormosil coating systems from the metal substrate

leaving a thin zincate product layer. $Na_2C_2O_4$ solutions were found to remove the LBL coating system and to provide corrosion protection of the underlying metal.

(a) Bare AA	**(b) LBL, $n = 15$, $t_i = 0$ h**	**(c) $t_i = 1$ h**
(d) $t_i = 2$ h	**(e) $t_i = 3$ h**	**(f) $t_i = 4$ h**
(g) $t_i = 5$ h		**(h) $t_i = 18$ h**

Figure 16: Removal of LBL Coatings from 2024-T3 Aluminum Alloy Using 0.1-M Sodium Oxalate Solution, pH = 6.8

III. References

1. Nylund, A. *Aluminum Transactions* **2000**, *2*, 121.

2   (a) Smith, C. J. E.; Baldwin, K. R.; Garrett, S. A.; Gibson, M. C.; Hewins, M. A. H.; Lane, P. L. *ATB Metallurgie* **1997**, *37*, 266. (b) Puippe, J. *Galvanotechnik.* **1990**, *90*, 3003. (c) Hinton, B. R. *Metal Finishing* **1991**, *89*, 15.

3. Twite, R. L.; Bierwagen, G. P. *Progress in Organic Coatings* **1998**, *33*, 91 (1998).

4. Roland, W.; Kresse, J. *ATB Metallurgie* **1997**, *37*, 89.

5. (a) Hinton, B. R. W. *J. Alloys Compd.* **1992** *180*, 15. (b) Arnott, D. R.; Ryan, N. E.; Hinton, B. R. W.; Sexton, B. A.; Hughes, A. E. *Appl. Surf. Sci.* **1985**, *22*, 236. (c) Morris, E.; Stoffer, J. O.; O'Keefe, T. J.; Yu, P.; Lin, X. *Polymeric Materials* **1999**, *81*, 167. (d) Ramanathan, L. V. *Corrosion Prevention & Control* **1998**, *4*, 87.

6. Schriever, M. P., U.S. Patent **5,551,994**, 3 September 1996.

7. (a) Danilidis, I.; Sykes, J. M.; Hunter, J. A.; Scamans, G. M. *Surf. Engr.* **1999**, *15*, 401. (b) Srinivasan, P. B.; Sathiyanarayanan, S.; Marikkannu, C.; Balakrishnan, K. *Corrosion Prevention & Control* **1995** (April), 35.

8. Rangel, C. M.; Simões, A.; Newman, R. C. *Portugaliœ Electrochimica Acta* **1997**, *15*, 383.

9. (a) Schram, T.; Goeminne, G.; Terryn, H.; Vanhoolst, W.; Van Espen, P. *Trans. I.M.F.* **1995**, *73*, 91. (b) Pearlstein, F.; Agarwala, V. S. *Plating and Surface Finishing* **1994**, *81*, 50.

10. van Ooij, W. J.; Zhang, C.; Zhang, J. W.; Yuan, W. *Electrochem. Soc. Proc.* **1998**, *97–41*, 222.

11. (a) van Ooij, W. J.; Song, J.; Subramanian, V. *ATB Metallurgie* **1997**, *37*, 137. (b) Child, T. F.; van Ooij, W. J., *Trans. IMF* **1999**, *77*, 64. (c) Subramanian, V.; van Ooij, W. J. *Surf. Engr.* **1999**, *15*, 168. (d) van Ooij, W. J; Child, T. *ChemTech* **1998**, *28*, 26.

12. Delaunois, F.; Poulain, V.; Petitjean, J. P. *ATB Metallurgie* **1997**, *37*.

13. (a) Schmidt, H. K. *Mater. Res. Soc. Symp. Proc.* **1990**, *180*, 961. (b) Mackenzie, J. D. *J. Sol–Gel Sci. Technol.* **1994**, *1*, 81.

14. Kasemann, R.; Schmidt, H. *New J. Chem.* **1994**, *18*, 1117.

15. (a) Kato, K. *J. Mater. Sci.* **1992**, *28*, 1445. (b) Kato, K. *J. Mater. Sci.* **1993**, *28*, 4033. (c) Donley, M. S.; Vreugdenhil, A. J. *J. Coat. Technol.* **2001**, *73*, 915. (d) Metroke, T. L.; Parkhill, R. L.; Knobbe, E. T. *Mater. Res. Soc. Symp. Proc.* **1999**, *576, 293*. (e) Metroke, T. L.; Knobbe, E. T. *Mater. Res. Soc. Symp. Proc.* **2000**, *628*, CC11.4.1. (f) Parkhill, R. L; Knobbe, E. T.; Donley, M. S. *Prog. Org. Coat.* **2001**, *41*, 261. (g) Osborne, J. H.; Blohowiak, K. Y.; Taylor, S. R.; Hunter, C.; Bierwagen, G.; Carlson, B.; Bernard, D.; Donley, M. S. *Prog. Org. Coat.* **2001**, *41*, 217. (g) Voevodin, N. N.; Grebasch, N. T.; Soto, W. S.; Kasten, L. S.; Grant, J. T.; Arnold, F. E.; Donley, M. S., *Prog. Org. Coat.* **2001**, *41*, 287. (h) Voevodin, N. N.; Grebasch, N. T.; Soto, W. S.; Arnold, F. E.; Donley, M. S., *Surf. Coat. Technol.* **2001**, *140*, 24. (i) Khobaib, M.; Reynolds, L. B.; Donley, M. S. *Surf. Coat. Techol.* **2001**, *140*, 16. (j) Yang, X. F.; Tallman, D. E.; Gelling, V. J.; Bierwagen, G. P.; Kasten, L. S.; Berg, J. *Surf. Coat. Technol.* **2001** *140*, 44. (k) Kachurina, O.; Metroke, T. L.; Stesikova, E.; Knobbe, E. T. *J. Coat. Technol.* **2002**, *74*, 43. (l) Metroke, T. L.; Kachurina, O.; Knobbe, E. T., *J. Coat. Technol.* **2002**, *74*, 53.

16.   Guglielmi, M. *J. Sol–Gel Sci. Technol.* **1997**, *8*, 443.

17.   Metroke, T. L.; Parkhill, R. L.; Knobbe, E. T. *Prog. Org. Coatings* **2001**, *41*, 233.

18.   (a) Klitzing, R.; Möhwald, H. *Thin Solid Films* **1996**, *284–285*, 352.   (b) Saremi, F.; Maassen, E.; Tieke, B. *Langmuir* **1995**, *11*, 1068.   (c) Klitzing, R.; Möhwald, H. *Macromolecules* **1996**, *29*, 6901.

19.   (a) Lvov, Y.; Haas, H.; Decher, G.; Mohwald, H.; Mikhailov, A.; Mtchedlishvivly, B.; Morgunova, E.; Vainstein, B. *Langmuir* **1994**, *10*, 4232.   (b) Lvov, Y.; Ariga, K.; Kunitake, T. *Chem. Lett.* **1994**, 2323.   (c) Onda, M.; Lvov, Y.; Ariga, K.; Kunitake, T. *Biotechnol. Bioeng.* **1996**, 51.   (d) Lvov, Y.; Ariga, K.; Ichinose, I.; Kunitake, T. *J. Am. Chem. Soc.* **1996**, *117*, 6117.   (e) Hodak, J.; Etchenique, R.; Calvo, E.; Singhal, K.; Bartlett, P. M. *Langmuir* **1997**, *13*, 2708.

20.   (a) Cheng, J. H.; Fou, A. F.; Rubner, M. F. *Thin Solid Films* **1994**, *244*, 985.   (b) Ferreira, M.; Cheung, J. H.; Rubner, M. F. *Thin Solid Films* **1994**, *244*, 806.

21.   Keller, S. W.; Kim, H. N.; Mallouk, T. E. *J. Am. Chem. Soc.* **1994**, *116*, 8817.

22.   (a) Zhang, X.; Gao, M.; Kong, X.; Sun, Y.; Shen, J. *J. Chem. Soc., Chem. Commun.* **1994**, 1055.   (b) Cooper, T. M.; Campbell, A. L.; Crane, R. L. *Langmuir* **1995**, *11*, 2713.   (c) Ichinoze, I.; Fujiyoshi, K.; Mizuki, S.; Lvov, Y.; Kunitake, T. *Chem. Lett.* **1996**, 257.

23.   (a) Keller, S. W.; Kim, H. N.; Mallouk, T. E. *J. Am. Chem. Soc.* **1994**, *116*, 8817.   (b) Feldheim, D. L.; Crabar, K. C.; Natan, M. J.; Mallouk, T. E. *J. Am. Chem. Soc.* **1996**, *118*, 7640.   (c) Schmitt, J.; Decher, G.; Dressik, W. J.; Branduo, S. L.; Geer, R. E.; Shashidhal, R.; Calvert, J. *Adv. Mater.* **1997**, *9*, 61.   (d) Freeman, R. G.; Grabar, K. C.; Allison, K. J.; Bright, R. M.; Davis, J. A.; Guthrie, A. P.; Hommer, M. B.; Jackson, M.

A.; Smith, P. C.; Walter, D. G.; Natan, M. J. *Science* **1995,** *267,* 1629. (e) Grabar, K. C.; Freeman, R. G.; Hommer, M. B.; Natan, M. J., *Anal. Chem.* **1995,** *67,* 735.

24.   Kotov, N. A.; Dékány, I.; Fendler, J. H. *J. Phys. Chem.* **1995,** *99,* 13065.

25.   (a) Kleinfeld, E. R.; Ferguson, G. S. *Chem. Mater.* **1995,** *7,* 2327. (b) Kleinfeld, E. R.; Ferguson, G. S. *Chem. Mater.* **1996,** *8,* 1575. (c) Kleinfeld, E. R.; Ferguson, G. S., Science, **1994,** *265,* 370. (d) Kleinfeld, E. R.; Ferguson, G. S. *Mater. Res. Soc. Symp. Proc.* **1995,** *369,* 697. (e) Lvov, Y.; Ariga, K.; Ichinose, I.; Kunitake, T. *Langmuir,* **1996,** *12,* 3038. (f) Kotov, N. A.; Dékány, I.; Fendler, J. H. *J. Phys. Chem.* **1995,** *99,* 13065. (g) Kotov, N. A.; Haraszti, T.; Turi, L.; Zavala, G.; Geer, R. E.; Dékány, I.; Fendler, J. H. *J. Am. Chem. Soc.* **1997,** *119,* 6821.

26.   Kotov, N. A.; Dékány, I.; Fendler, J. H. *Adv. Mater.,* **1996,** *8,* 637.

27.   Kleinfeld, E. R.; Ferguson, G. S. *Science* **1994,** *265,* 370.

28.   Kotov, N. A.; Haraszti, T.; Zavala, G.; Geer, R. E.; Dékány, I.; Fendler, J. H. *J. Am. Chem. Soc.* **1997,** *119,* 6821.

29.   Schriever, M. P. U.S. Patent **5,873,953,** 2 February 1999.

30.   Jones, D. A., Ed. *Principles and Prevention of Corrosion* (New York: Macmillan Publishing Co., 1992).

31.   Twite, R.; Balbyshev, S.; Bierwagen, G. *Spec. Pub. Electrochem. Soc.* **1997** *95–16* (*Proceedings of the Symposium on Environmentally Acceptable Inhibitors and Coatings*), 202.

32.   Ilevbare, G. O.; Scully, J. R.; Yuan, J.; Kelly, R. G. *Corrosion* **2000,** *56.*

33.   Bacon, R. C.; Smith, J. J.; Rugg, F. M. *Ind. Eng. Chem.* **1948,** *40,* 161.

34.   Zhang, S.; Czekaj, C. L.; Ford, W. T. *J. Magn. Reson.* **1994**, *A111*, 87.

35.   Correa-Duarte, M. A.; Giersig, M.; Kotov, N. A.; Liz-Marzan, L. M. *Langmuir* **1998**, *14*, 6430.

36.   Kotov, N. A.; Haraszti, T.; Turi, L.; Zavala, G.; Geer, R. E.; Dékány, I.; Fendler, J. H. *J. Am. Chem. Soc.* **1997**, *119*, 6821.

37.   Delattre, L.; Dupuy, C.; Babonneau, F. *J. Sol–Gel Sci. Technol.* **1994**, *2*, 185.

38.   (a) Ilevbare, G. O.; Scully, J. R.; Yuan, Y.; Kelly, R. G. *Corrosion* **2000**, *56*, 227. (b) Hughes, A. E.; Taylor, R. J.; Hinton, B. R. W. *Surf. Interface Anal.* **1997**, *25*, 223. (c) Lytle, F. W.; Greegor, R. B.; Bibbins, G. L.; Blohowiak, K. Y.; Smith, R. E.; Tuss, G. D. *Corr. Sci.* **1995**, *37*, 349. (d) Jeffcoate, S.; Isaacs, H. S.; Aldykiewicz, A. J.; Ryan, M. P. *J. Electrochem. Soc.* **2000**, *147*, 540. (e) Xia, L.; McCreery, R. L. *J. Electrochem. Soc.* **1998**, *15*, 3083.

39.   Levela, L.; Chin, J.; del Amo, B. *Prog. Org. Coat.* **1999**, *36*, 211.

40.   Dai, J.; Sullivan, D. M.; Bruening, M. L. *Ind. Eng. Chem. Res.* **2000**, *39*, 3528.

41.   Kotov, N. A.; Magonov, S.; Tropsha, E. *Chem. Mater.* **1997**, *9* (3), 1345.

42.   Kobotiatis, L.; Pebere, N.; Koustsousoukos, P. *Corr. Sci.* **1999**, *41*, 941.